Biochimica et Biophysica Acta 1853 (2015) 2464–2480

Contents lists available at ScienceDirect

Biochimica et Biophysica Acta

journal homepage: www.elsevier.com/locate/bbamcr

Different states of integrin LFA-1 aggregation are controlled through its association with tetraspanin CD9

Raquel Reyes [a,b], Alicia Monjas [a], María Yánez-Mó [c,d], Beatriz Cardeñes [a], Giulia Morlino [e], Alvaro Gilsanz [a], Yesenia Machado-Pineda [a], Esther Lafuente [f], Peter Monk [g], Francisco Sánchez-Madrid [e,h], Carlos Cabañas [a,f,*]

[a] Centro de Biología Molecular Severo Ochoa (CSIC-UAM), 28049 Madrid, Spain
[b] Departamento de Biología, Facultad de Ciencias, Universidad Autónoma de Madrid, 28049 Madrid, Spain
[c] Unidad de Investigación, Hospital Santa Cristina, Instituto de Investigación Sanitaria La Princesa (IIS-IP), 28006 Madrid, Spain
[d] Departamento de Biología Molecular, Facultad de Ciencias, Universidad Autonoma de Madrid, 28049 Madrid, Spain.
[e] Departamento de Biología Vascular e Inflamación, Centro Nacional de Investigaciones Cardiovasculares (CNIC), 28029 Madrid, Spain
[f] Departamento de Microbiología I, Area de Inmunología, Facultad de Medicina, Universidad Complutense de Madrid, 28040 Madrid, Spain
[g] University of Sheffield Medical School, Sheffield S10 2RX, UK
[h] Servicio de Inmunología, Hospital de la Princesa, Instituto de Investigación Sanitaria La Princesa (IIS-IP), 28006 Madrid, Spain

ARTICLE INFO

Article history:
Received 11 September 2014
Received in revised form 11 May 2015
Accepted 14 May 2015
Available online 21 May 2015

Keywords:
Tetraspanin
Integrin
CD9
LFA-1
Adhesion
Cytotoxicity

ABSTRACT

The tetraspanin CD9 has been shown to interact with different members of the β1 and β3 subfamilies of integrins, regulating through these interactions cell adhesion, migration and signaling. Based on confocal microscopy co-localization and on co-immunoprecipitation results, we report here that CD9 associates with the β2 integrin LFA-1 in different types of leukocytes including T, B and monocytic cells. This association is resistant to stringent solubilization conditions which, together with data from chemical crosslinking, *in situ* Proximity Ligation Assays and pull-down experiments, suggest a primary/direct type of interaction mediated by the Large Extracellular Loop of the tetraspanin. CD9 exerts inhibitory effects on the adhesive function of LFA-1 and on LFA-1-dependent leukocyte cytotoxic activity. The mechanism responsible for this negative regulation exerted by CD9 on LFA-1 adhesion does not involve changes in the affinity state of this integrin but seems to be related to alterations in its state of aggregation.

1. Introduction

The β2 subfamily of integrins comprises four distinct members, αLβ2, αMβ2, αXβ2, and αDβ2, that are selectively expressed on leukocytes (for review [15,28,33]). The integrin αLβ2, also termed LFA-1 (Lymphocyte Function-associated Antigen-1) or CD11a/CD18 antigen, is expressed on most types of leukocytes and primarily on lymphocytes, whereas expression of the rest of members of this subfamily is rather restricted to myeloid cells. LFA-1 interacts with intercellular adhesion molecules (ICAM-1, -2, or -3), playing a pivotal role in many crucial leukocyte functions that require intercellular adhesion, such as extravasation into tissues, organization of the immune synapse and antigen presentation, inter-lymphocyte collaboration and killing of target cells by CTL or NK cells [2,40,63,66].

LFA-1 can exist in different states of activation regarding its ability to bind ligands. Resting T lymphocytes express LFA-1 with low affinity and avidity for ligands, necessary for their normal circulation in the blood as individual cells. However, activation by the TCR-CD3 complex or receptors for different cytokines and chemokines, results in rapid activation of LFA-1 enabling T cells to adhere to other cells [15,27,72]. Activation of LFA-1 can be induced through changes in the affinity of individual integrin molecules, reflecting conformational alterations, or through changes in the valency of interactions with multivalent ligands [18]. In terms of ligand binding affinity, at least three different conformational states of LFA-1 have been identified: a bent conformation of low affinity, an extended conformation with closed headpiece displaying intermediate affinity, and a high affinity extended conformation with open headpiece and separated intracellular tails [18,39]. PMA induces the intermediate affinity state but also increases the diffusion of LFA-1 molecules on the cell surface, which in the presence of multivalent ligand, leads to aggregation/clustering of this integrin [18,42]. On the other hand, extracellular Mn^{2+} induces the high affinity conformation of LFA-1 [18,26] but also induces changes in the local density (i.e. the

* Corresponding author at: Centro de Biología Molecular Severo Ochoa (CSIC-UAM), Nicolás Cabrera 1, 28049 Madrid, Spain. Tel.: +34 911964513; fax: +34 911964420.
E-mail address: ccabanas@cbm.csic.es (C. Cabañas).

http://dx.doi.org/10.1016/j.bbamcr.2015.05.018
0167-4889/

clustering) of integrin molecules, which is reflected by changes in the number of effective adhesive bonds (i.e. the valency) with ligand [19,55].

CD9 is a member of the tetraspanin family of integral membrane proteins [20,77] abundantly expressed on the surface of endothelial cells, some leukocytes and many types of tumor cells [21,36,64]. CD9 was initially characterized as a lympho-hematopoietic marker [14] and received the name "Motility-Regulatory Protein" (MRP) [49]. CD9 has been also implicated in the formation and maintenance of muscular myotubes [68], in nervous cell neurite outgrowth [61], and in sperm–oocyte fusion [23]. Like other tetraspanins, CD9 associates on the cell surface with different integrins and many of the functional effects that have been attributed to CD9 may be indeed related to its ability to associate to integrin molecules [6,7].

Functional interactions of CD9 with several members of the β1 and β3 subfamilies of integrins have been reported, usually based on the effects exerted by CD9-specific mAbs on the associated integrin-dependent adhesion, migration and signaling (reviewed in [6,7]). However, to our knowledge, only one published report includes some indication – merely based on co-immunoprecipitation evidence – suggestive of a possible interaction between CD9 and the β2 integrin subunit [69], although this study did neither address the type or functional aspects of this interaction. In addition, functional association of LFA-1 with tetraspanins CD81 (the most closely related to CD9) and CD82, has been described on T lymphocytes [62,75], which prompted us to investigate in more detail whether CD9 is also functionally associated with the β2 integrin LFA-1 on leukocytes.

We report here that CD9 associates directly with LFA-1 in different types of leukocytes and exerts inhibitory effects on its adhesive capacity and on leukocyte LFA-1-dependent cytotoxic activity.

2. Materials and methods

2.1. Cells and cell cultures

Primary T lymphoblasts were obtained from peripheral blood mononuclear cells from healthy donors treated with 5 μg/ml phytohemagglutinin (Amersham Biosciences) for 48 h, as described previously [25,48]. Cells were then cultured for 7–10 days in RPMI-1640 containing 10% FBS and 50 U/ml IL-2 (Eurocetus). HSB-2 and Jurkat (T cell lines), JY and Daudi (B cell lines) and THP-1 and U937 cells (monocytic cell lines) were cultured in RPMI-1640 supplemented with 10% FBS, antibiotics and glutamine. THP-1 and U937 differentiation into macrophage-like cells was induced with PMA (100 ng/ml) for 24 h.

2.2. Expression constructs and RNA silencing transfection

For stable transfection experiments, HSB-2 and U937 cells were electroporated with 20 μg pcDNA3-CD9 plasmid at 200 V (2 × 10 ms pulses in a 0.4 cm electroporation cuvette) using an ECM830 BTX electroporation system and selected with 1 mg/ml G418. For CD9 silencing, Jurkat cells were retroviraly transduced (OriGene Technologies) with the shRNA-coding plasmids TI356235 (the plasmid with the CD9 shRNA cassette insert) and TR20003 ("TR2" control plasmid without shRNA insert), according to manufacturer's indications and selected with 1 μg/ml puromycin.

2.3. Antibodies and reagents

ICAM-1-Fc chimeric protein consisting of the five domains of ICAM-1 fused to the Fc region of human IgG1 was prepared as described [9]. Anti-β-tubulin antibody was purchased from Sigma and the anti-CD18 biotin-conjugated antibody (MEM-48) from ImmunoTools. The antibodies anti-β2 integrin Lia3/2 [17] and TS1/18 [58], anti-αL TP1/40 [17] and TS1/11 [58], anti-αM Bear-1 [41] and anti-αX HC1/1 [16], anti-CD9 VJ1/20 [78], PAINS-10 and PAINS-13 [31], anti-CD147 VJ1/9 and anti-CD59 VJ1/12 [78] and anti-HSPA8 PAINS-18 [29,31] were purified by protein A or protein-G affinity chromatography. The anti-CD81 5A6 mAb was kindly provided by Dr. Shoshana Levy (Stanford University School of Medicine, USA), the β2 stimulatory mAb KIM185 by Dr. Martyn K. Robinson (UCB-Celltech., Slough, UK), the anti-CD105 mAb P4A4 by Dr. Carmelo Bernabeu (CIB-CSIC, Madrid, Spain) and the anti-β2 mAb m24 by Dr. Nancy Hogg (Cancer Research UK, London, UK).

2.4. Flow cytometry analysis

For protein surface expression analysis cells were washed twice in RPMI-1640, incubated with primary antibodies at 4 °C for 30 min, followed by FITC-conjugated anti-mouse IgG (Sigma) and fixed in 2% formaldehyde in PBS. For flow cytometric analysis of m24 epitope expression, HSB-2 and JK cells were washed in cation-free PBS and incubated for 15 min at 37 °C with Mn^{2+} (10, 20, 40, 100 and 400 μM) or with Ca^{2+}/Mg^{2+} (0.5 mM and 1 mM respectively) in the presence of mAb 24 (5 μg/ml), washed and stained with secondary FITC-anti-mouse IgG. Fluorescence was measured using a FACScanTM flow cytometer (Beckton–Dickinson).

2.5. Immunofluorescence, confocal and TIRF microscopy

For immunofluorescence studies cells, treated or not with 0.4 mM Mn^{2+} for 20 min at 37 °C, were seeded on 12-mm glass coverslips coated with poly-L-lysine (50 μg/ml). Cells were fixed in 2% paraformaldehyde, blocked in 1% BSA in TBS and incubated for 1 h with TS1/11 or TS1/18 mAbs (10 μg/ml), followed by secondary antibody Alexa FluorTM-594 anti-mouse IgG (Invitrogen), rabbit polyclonal anti-CD9 antibody H-110 (Santa Cruz Biotechnology) and Alexa FluorTM-488 anti-rabbit IgG (Invitrogen). For THP-1 cells, Fc receptors were saturated with human gammaglobulin for 30 min, prior to fixation. Samples were mounted with Mowiol reagent (Calbiochem) and images were obtained with a Zeiss LSM510 Meta inverted microscope. Fluorescence co-localization histograms and Pearson coefficient values were obtained using the Fiji plug-in "Intensity correlation analysis" [47,60]. Fiji software was also used for setting the threshold and for detection and quantitation of fluorescent objects.

For TIRF (total internal reflection fluorescence) miscroscopy, JK TR2 and JK shCD9 cells were first activated with PMA (200 ng/ml for 2 h), then plated onto ICAM-1-Fc-coated (14 μg/ml) 35 mm Petri dishes with glass bottom (2.5×10^5 cells/plate), and incubated for 90 min at 37 °C to allow adhesion. After washing non-adhered cells with PBS, adhered cells were fixed in 2% paraformaldehyde (10 min, room temperature) and then permeabilized with 0.3% Triton-X100 in TBS buffer. Immunofluorescence staining of beta-2 integrin with mAb TS1/18 was performed as described above, and images were obtained with an inverted Olympus Xcellence IX83P2ZF TIRF miscroscopy system. Fiji software was used for setting the threshold and for detection and quantitation of fluorescence in clusters.

2.6. Co-immunoprecipitations

Co-immunoprecipitation experiments were performed using intact cells, in order to detect only surface protein–protein interactions. Cells were incubated for 15 min at 37 °C (or for 60 min at 4 °C in parallel control experiments) with the specific TS1/18 (anti-β2) or VJ1/20 (anti-CD9) or control anti-CD105 and anti-CD59 antibodies in the presence of 0.5 mM Ca^{2+}/1 mM Mg^{2+}, followed by washing the antibody excess. Cells were then lysed for 15 min at 4 °C in TBS containing 1% Brij-97 or 1% Triton-X100 in the presence of corresponding extracellular cations and protease inhibitors and, after removal of insoluble material, incubated overnight at 4 °C with protein G-sepharose. Beads were then washed with 1:5 diluted lysis buffer, boiled in nonreducing Laemmli buffer, resolved by 8% (for β2 detection) or 12% (for CD9)

SDS-PAGE and transferred onto nitrocellulose membranes. Membranes were then blocked with 3% BSA and developed with the β2 (MEM-48) or CD9 (VJ1/20) biotin-conjugated antibodies followed by streptavidin HRP (Thermo scientific) and ECL-chemiluminescence.

2.7. Covalent chemical cross-linking

THP-1/PMA and JY cells were extracted in 1% Brij97 lysis buffer (containing 20 mM Hepes,150 mM NaCl, 0.5 mM $CaCl_2$, 3 mM $MgCl_2$ and protease inhibitors), pH 7.4. After removal of insoluble material, lysates were treated with 0.25 mM thiol-cleavable cross-linker 3,3′-dithiobis(sulfosuccinimidylpropionate) (DTSSP) for 30 min at 4 °C. The cross-linking reaction was quenched for 15 min at room temperature with 10 mM glycine, pH 7.4, and then Triton X-100 was added to a final concentration of 1% (v/v) to cross-linked lysates and to parallel non-cross-linked lysates used as controls. Samples were immunoprecipitated with anti-β2 integrin mAb TS1/18, with anti-CD9 mAb VJ1/20 or with anti-CD9 pAb (H110), as indicated, resolved by SDS-PAGE either under reducing conditions (to break the thiol bond in DTSSP-crosslinked protein complexes) or under non-reducing conditions and subsequent immunoblotting with biotinylated anti-CD9 (VJ1/20) or anti-β2 integrin (MEM-48) mAbs, followed by streptavidin-HRP (Thermo Scientific) and ECL-chemiluminescence.

2.8. Pull-down assays

GST-fusion proteins containing the LEL region from human wt CD9, wt CD81 and wt CD63 were prepared as previously described [4,32,37]. JY and THP-1 cells were washed three times in PBS and either left untreated or their surface proteins biotinylated with 1 mM EZ-Link^R Sulfo-NHS-LC-Biotin (Thermo Scientific) in PBS with 1 mM $CaCl_2$, 1 mM $MgCl_2$ for 30 min at 4 °C. Cells were then washed twice in PBS + 100 mM glycine to quench and remove excess biotin. Biotinylated and non-biotinylated cells were lysed in 1% Brij-97 or in 1% Triton-X100 buffer and incubated overnight at 4 °C with equal amounts of GST-fusion proteins, pulled down with glutathione-agarose for 3 h at 4 °C, washed in 1:10 diluted lysis buffer and boiled in non-reducing Laemmli buffer. For non-biotinylated cells, the presence of β2 integrin in the pulled-down complexes was revealed by immunoblotting with biotinylated mAb MEM-48 and detection with streptavidin-HRP and ECL-chemiluminescence. The levels of pulled-down GST-fusion proteins were assessed by western-blot using an anti-GST rabbit polyclonal antibody (Santa Cruz Biotechnology). For surface-biotinylated cells, all lysate proteins pulled-down by GST or by LEL–GST–CD9 were isolated with glutathione-sepharose beads and detected with streptavidin-HRP and ECL-chemiluminescence.

2.9. Cell adhesion assays

Static cell adhesion to ICAM-1-coated dishes was performed as described elsewhere [29,54]. 96-well flat-bottom plates were pre-coated with 6 μg/ml (for THP-1/PMA and T-lymphoblast cells) or 12 μg/ml (for JY, HSB2 and JK cells) of ICAM-1-Fc and blocked with 1% BSA. For PMA-stimulated cell adhesion, cells were incubated with 50 or 200 ng/ml of PMA in RMPI-1640 for 2 h at 37 °C. Cells were loaded with the fluorescent probe BCECF-AM (Sigma) and added (2×10^5 cells/well) in adhesion medium (Hepes 20 mM, NaCl 149 mM, 2 mg/ml glucose), stimulated with 0.5 mM Ca^{2+}/1 mM Mg^{2+} or 20–400 μM Mn^{2+} and incubated for 20–60 min at 37 °C. When indicated, 20 μg/ml of anti-CD9 (VJ1/20, PAINS-10 and PAINS-13), anti-β2 (Lia3/2 and KIM185) or the control anti-HSPA8 (PAINS-18) mAbs were pre-incubated with cells for 15 min at 4 °C before transferring the plates to 37 °C. The plates were then washed by gravity with warm PBS for 20 min at 37 °C. The percentage of adherent cells was calculated by determining their fluorescence in a microplate reader (TecanGENios), considering as 100% the total fluorescence of cells before washing. For determining cell adhesion under flow conditions, JK TR2 and JK shCD9 cells were first activated with PMA (100 ng/ml for 1 h) and labeled with CFSE or CMAC fluorescent probes and allowed to adhere for 15 min at 37 °C to immobilized ICAM-1 (5 μg/ml). Shear stress was started at 0.5 dyn/cm^2 and increased up to 20 dyn/cm^2 at 1 min intervals. Cell detachment was calculated by normalizing the number of adhered cells relative to the number of cells observed at the minimal flow rate of 0.5 dyn/cm^2.

2.10. Lymphokine-activated killer cell assay

The LAK cell assay was performed essentially as described [30,53] with 4×10^4 Daudi cells/well as targets and 4×10^5 T lymphoblasts as effector cells [25] in triplicates in 96-well U-bottom plates in a final volume of 200 μl. For antibody inhibition studies, purified mAbs were used at 50 μg/ml. Then the plates were incubated at 37 °C for 5 h and the percentage of specific target cytolysis was determined from the amount of LDH activity, measured as INT reduction, in the culture supernatant. 20 μl of lactate solution (Sigma, 36 mg/ml in 10 mM Tris buffer, pH 8.5) was added to the cell-free supernatant, followed by addition of 20 μl INT solution (Sigma, 2 mg/ml in PBS) and 20 μl of a solution containing NAD^+/diaphorase (NAD^+: Sigma, 3 mg/ml; diaphorase: Boehringer, 13.5 U/ml; BSA: 0.03%; sucrose: 1.2%; in PBS) and incubated for 20 min. The reaction was terminated with 20 μl of the LDH inhibitor oxamate (Sigma, 16.6 mg/ml in PBS) and the absorbance at 492 nm was determined in a microplate reader.

2.11. In situ proximity ligation assays

In situ proximity ligation assays (PLAs) (Duolink kit, Olink Bioscience, Uppsala, Sweden) allows detection of direct or closely proximal protein–protein interactions in cell samples by fluorescence microscopy [65,76]. THP-1/PMA cells were seeded, fixed and blocked as described above. Next samples were incubated simultaneously with mouse mAbs anti-β2 TS1/18, anti-αL TS1/11, anti-CD147 VJ1/9 or anti-CD81 5A6 mAbs, and with the anti-CD9 H-110 rabbit polyclonal antibody (sc-9148, Santa Cruz Biotechnology), followed by specific oligonucleotide-labeled secondary antibodies (anti-mouse-plus probe and anti-rabbit minus probe). Only if the two different target proteins are in close proximity (≤40 nm), the oligonucleotides of the two probes will hybridize and after a rolling-circle amplification reaction and detection with a different fluorescently labeled oligonucleotide a fluorescent dot signal can be visualized and analyzed by microscopy.

2.12. Statistical analysis

One-factor ANOVA analysis was performed using the statistics software SPSS (IBM). The data distribution was tested for normality by Bonferroni test.

Fig. 1. CD9 co-localizes with LFA-1 on THP-1 cell surface. A) Flow cytometric detection of CD9 (mAb VJ1/20), β2 (mAb TS1/18), αL (mAb TP1/40), αM (mAb Bear-1), αX (mAb HC1/1) and CD147 (mAb VJ1/9) proteins on the surface of THP-1 monocytic cells or THP-1/PMA macrophage-like cells. Gray filled histograms correspond to negative controls; empty histograms correspond to the expression of the indicated molecules. The numbers in boxes represent M.F.I. values. B) and C) confocal microscopy of THP-1, THP-1 in the presence of 0.4 mM Mn^{2+} and THP-1/PMA differentiated cells showing in panel B co-localization of CD9 (green) and β2 (red) and in panel C co-localization of CD9 (green) and αL (red) at the cell surface. Representative images of confocal sections for each channel (green and red) and merged channels are shown together with co-localization histograms (right panels) showing Pearson co-localization values. Scale bars = 5 μm.

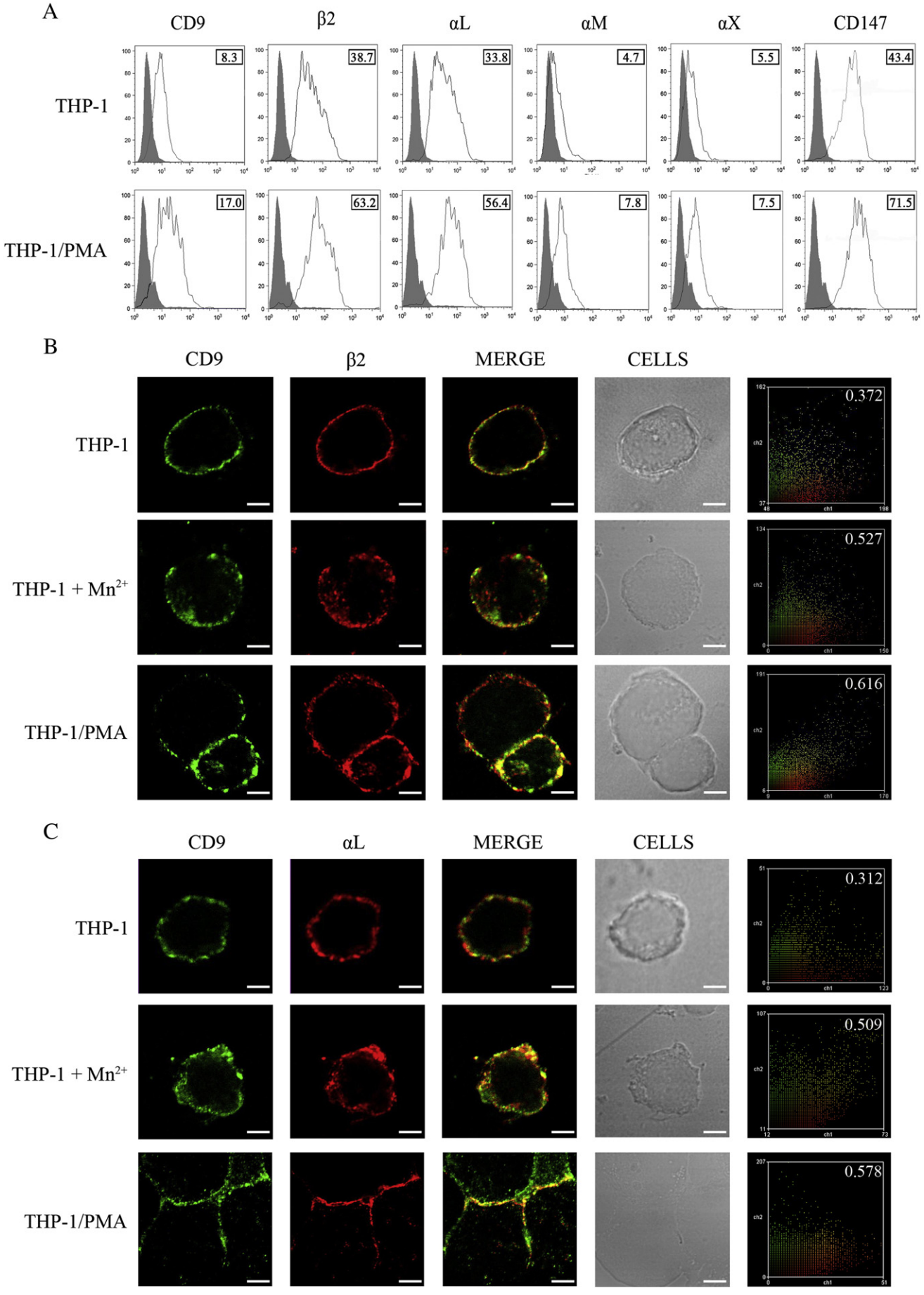
A
CD9
β2
αL
αM
αX
CD147
THP-1
8.3
38.7
33.8
4.7
5.5
43.4
THP-1/PMA
17.0
63.2
56.4
7.8
7.5
71.5
B
CD9
β2
MERGE
CELLS
THP-1
0.372
THP-1 + Mn2+
0.527
THP-1/PMA
0.616
C
CD9
αL
MERGE
CELLS
THP-1
0.312
THP-1 + Mn2+
0.509
THP-1/PMA
0.578

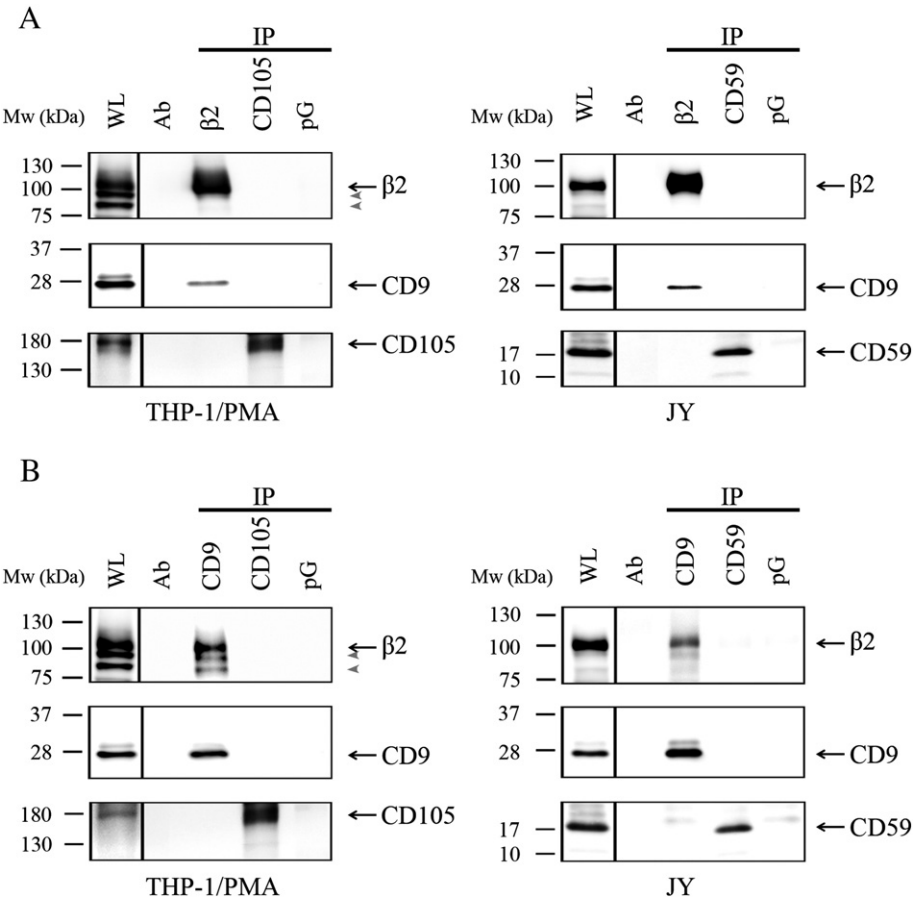

Fig. 2. Co-immunoprecipitation analysis of the association between LFA-1 and CD9. THP-1/PMA (left panels) and JY (right panels) cells were incubated with the immunoprecipitating mAbs TS1/18 (anti-β2) in panel A, and VJ1/20 (anti-CD9) in panel B, prior to their lysis in 1% Brij-97-containing lysis buffer. Protein immunocomplexes were precipitated with protein-G-sepharose, then resolved by 8% (for detection of β2) or 12% (for detection of CD9) SDS-PAGE under non-reducing conditions, and immunoblotted with anti-β2 (MEM-48) (upper panels) or anti-CD9 (VJ1/20) (middle panels) biotin-conjugated mAbs or with anti-CD105 or anti-CD59 control proteins (lower panels). Blots are representative of three different experiments. In some cell lysates, several β2 bands (indicated by gray arrowheads), probably corresponding to differences in glycosylation or partial degradation, are immunodetected. WL: whole cell lysate. pG: protein-G-sepharose without precipitating antibody.

3. Results

3.1. CD9 associates with β2 integrin on the leukocyte surface

To investigate the possible association between CD9 and the β2 integrin LFA-1, we first studied the co-localization of these molecules by double immunofluorescence staining with specific mAbs and confocal microscopy analysis. We employed monocytic THP-1 cells because they constitutively display detectable surface expression of the three major β2 integrins ($\alpha_L\beta_2$, $\alpha_M\beta_2$ $\alpha_X\beta_2$) and CD9 (Fig. 1A, upper histograms). Confirming previous reports, we observed that the surface expression of both CD9 [32,50] and β2 integrins [1] was increased during PMA-induced differentiation of THP-1 cells into macrophage-like cells (Fig. 1A, lower histograms). As shown in Fig. 1B, CD9 and β2 integrin subunit were found to co-localize partially on the surface of undifferentiated monocytic THP-1 cells and this co-localization became much more evident on PMA-differentiated macrophage-like THP-1 (THP-1/PMA) cells, particularly at the cell–cell contact regions in the

Fig. 3. Direct interaction of CD9 and LFA-1 at the cell surface is mediated by the Large Extracellular Loop of CD9. A) THP-1/PMA or JY cells were lysed with 1% Triton-X100-based lysis buffer after incubation with immunoprecipitating mAbs TS1/18 (anti-β2) or VJ1/20 (anti-CD9). Immunoblotting of co-immunoprecipitated proteins was performed as described in Materials and methods. WL: whole cell lysate. pG: protein-G-sepharose without precipitating antibody. B) 1% Brij-97 extracts of JY cells were treated with DTSSP cross-linker and Triton X-100 was then added to a final concentration of 1% (v/v) to cross-linked lysates and to parallel non-cross-linked lysates used as controls, as indicated. Samples were immunoprecipitated with anti-β2 integrin mAb TS1/18 (as indicated in the left panel and lanes 1 and 2 in the right panel) or with anti-CD9 mAb VJ1/20 (lanes 3 and 4 in the right panel), resolved by SDS-PAGE either under reducing conditions to break the thiol bond in DTSSP-crosslinked protein complexes (left panel) or under non-reducing conditions (right panel) and subsequently immunodetected with biotinylated anti-CD9 (VJ1/20) or anti-β2 integrin (MEM-48) mAbs. C) *In situ* proximity ligation assays (PLAs) were performed on THP-1/PMA macrophage-like cells as described in Materials and methods. Red fluorescent dots reveal molecular interactions between CD9 and β2 or αL integrin subunits of LFA-1. The interactions between CD147/CD9 and CD81/CD9 are also shown as negative and positive controls, respectively (left panels). Maximal projections of representative confocal stacks are shown. Scale bars = 5 μm. The right panel shows the quantitation of total fluorescence per cell. ***$p < 0.001$. D) Non biotinylated (left panel) or surface-biotinylated (right panel) JY cells were lysed in Triton-X100-based buffer and incubated with the LEL-GST constructs of human CD81 or CD9, as indicated. The GST and CD63–LEL–GST constructs were used as negative controls for specificity of binding. Formed complexes were pulled-down with glutathione-sepharose beads. For non-biotinylated cells, the presence of β2 integrin in the pulled-down complexes was revealed by immunoblotting with mAb MEM-48 (upper left-panel) and loading controls of GST fusion proteins stained with anti-GST polyclonal antibody are also shown (lower left-panel). For surface-biotinylated cells, all lysate proteins pulled-down by GST, CD63–LEL–GST or by CD9–LEL–GST were isolated with glutathione-sepharose beads and detected with streptavidin-HRP. As a control, β2 integrin was also immunoprecipitated with mAb TS1/18 from 1% Triton-X100 lysates of either surface-biotinylated or non-biotinylated (NB) JY cells and detected with streptavidin-HRP (which also clearly reveals the accompanying biotinylated 185 kDa band corresponding to the αL subunit of LFA-1) or by immunodetection with anti-β2 mAb MEM48, respectively.

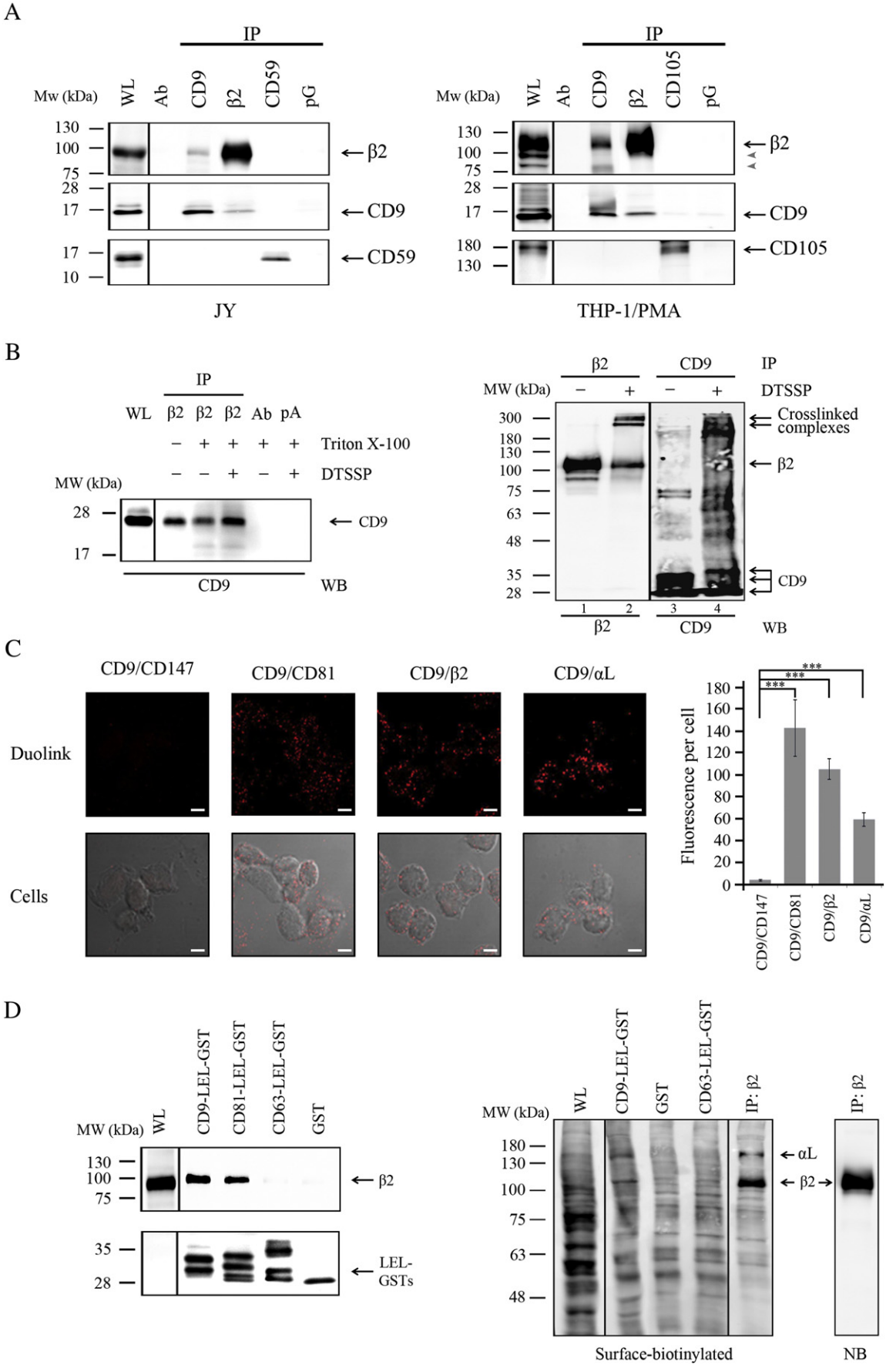
A
IP
Mw (kDa)
WL
Ab
CD9
β2
CD59
pG
130
100
75
28
17
17
10
← β2
← CD9
← CD59
JY
IP
Mw (kDa)
WL
Ab
CD9
β2
CD105
pG
130
100
75
28
17
180
130
← β2
← CD9
← CD105
THP-1/PMA
B
IP
WL β2 β2 β2 Ab pA
− + + + + Triton X-100
− − + − + DTSSP
MW (kDa)
28
17
← CD9
CD9
WB
β2 CD9 IP
MW (kDa) − + − + DTSSP
300
180
130
100
75
63
48
35
28
Crosslinked complexes
← β2
CD9
1 2 3 4
β2 CD9 WB
C
CD9/CD147
CD9/CD81
CD9/β2
CD9/αL
Duolink
Cells
Fluorescence per cell
***
***
***
180
160
140
120
100
80
60
40
20
0
CD9/CD147
CD9/CD81
CD9/β2
CD9/αL
D
MW (kDa)
WL
CD9-LEL-GST
CD81-LEL-GST
CD63-LEL-GST
GST
130
100
75
35
28
← β2
← LEL-GSTs
MW (kDa)
WL
CD9-LEL-GST
GST
CD63-LEL-GST
IP: β2
IP: β2
180
130
100
75
63
48
← αL
← β2
Surface-biotinylated
NB

cellular aggregates that form during this differentiation process, as indicated by the increase in the Pearson co-localization coefficient. As we reported previously [55], when activation of β2 integrin was induced with extracellular divalent cation Mn^{2+} the localization of β2 integrin molecules changed from an evenly-distributed pattern to a patched/clustered distribution and interestingly CD9 was clearly found co-localizing with clustered β2 integrin. Since the β2-specific mAb stained all the β2-containing integrins we also performed double immunofluorescence using an αL-specific mAb, confirming the pattern of co-localization between CD9 and LFA-1 (Fig. 1C). The specificity of the co-localization between CD9 and LFA-1 was evidenced by the almost complete lack of co-localization observed between CD9 and CD147 (Supplementary Fig. 1), which is another abundantly expressed surface protein on these cells (Fig. 1A).

Similar co-localization results were also observed in other leukocytes, including the B lymphoblastic JY and T leukemic Jurkat cells, which only express LFA-1, but not $\alpha_M\beta_2$ or $\alpha_X\beta_2$ (Supplementary Fig. 2), and collectively suggest that CD9 associates with β2-integrins, and particularly with LFA-1 ($\alpha_L\beta_2$), on the surface of different types of leukocytic cells.

To confirm the association of CD9 with LFA-1, co-immunoprecipitation experiments were performed using JY and THP-1/PMA cells. All immunoprecipitations were performed using intact cells that were incubated with the immunoprecipitating mAbs at 37 °C prior to their lysis, thus ensuring that only interactions between cell surface molecules were detected. Immunoprecipitation using the β2-specific mAb TS1/18, from Brij-97 lysates of THP-1/PMA and JY cells, followed by immunoblotting with anti-CD9 mAb VJ1/20 clearly showed that this tetraspanin was co-precipitated with integrin LFA-1 (Fig. 2A). Co-immunoprecipitation was also detected in the reverse order, i.e. immunoprecipitating CD9 followed by immunodetection of β2 integrin (Fig. 2B). Moreover, the association of LFA-1 with CD9 observed in Brij97-based lysates of THP-1/PMA and JY cells persisted under more stringent solubilization conditions such as the use of detergent Triton-X100 (1.0 %) (Fig. 3A), thus pointing to a strong/direct type of interaction taking place between these molecules on the leukocyte surface. Similar results were also obtained using Triton-X100 (1.0 %) lysates of Jurkat cells (not shown). Parallel immunoprecipitations were also carried out with cells incubated with immunoprecipitating antibodies at 4 °C and subsequently lysed in Triton-X100, to rule out that the observed association between CD9 and β2 integrin is caused by pre-incubation with antibodies at 37 °C (Supplementary Fig. 3), and also with cells lysed at 4 °C with this detergent prior to the addition of precipitating antibodies, yielding essentially the same results (data not shown).

When chemical crosslinking of solubilized proteins from JY cells was performed with thiol-cleavable DTSSP an important increase in the amount of CD9 co-immunoprecipitated with β2 integrin could be detected after cleavage of the cross-linked protein complexes in reducing conditions (Fig. 3B, left panel). Essentially the same results were also obtained with THP-1/PMA cells (data not shown). Furthermore, immunoprecipitation with anti-β2 and anti-CD9 mAbs of non-cleaved cross-linked protein complexes resolved under non-reducing conditions clearly showed high molecular weight complexes of around 300 kDa which were immunodetected both with anti-β2 and anti-CD9 antibodies (Fig. 3B, right panel), indicating that these molecules had been directly cross-linked. It is worth indicating that these ~300 kDa bands are compatible with covalently cross-linked complexes containing both LFA-1 subunits (αL = 185 kDa; β2 = 95 kDa) plus a molecule of CD9 (24 kDa). Definitive proof that these ~300 kDa bands correspond to complexes including CD9 and β2 integrin, was provided by the fact that they were immunoprecipitated both with anti-β2 and anti-CD9 antibodies, and immunodetected in both cases with an anti-β2 antibody (MEM-48) (Supplementary Fig. 4). Taken together, these crosslinking experiments support a direct-type of interactions occurring between endogenous LFA-1 and CD9 in leukocytic cells.

Further support for the direct nature of CD9–LFA-1 interaction on the leukocyte surface was provided by *in situ* Proximity Ligation Assays (PLAs) on non-permeabilized THP1/PMA cells. PLA signal is only detected when the secondary probes directed against the two different molecules whose interaction is suspected are within a short range distance (<40 nm) compatible with direct or closely proximal molecular interactions. As shown in Fig. 3C, PLA signal between CD9 and both subunits of LFA-1 (α_L and β_2) was clearly revealed on the surface of THP-1/PMA cells, being the PLA signal particularly evident at cell–cell contact regions. The same procedure with the abundantly expressed membrane molecule CD147/EMMPRIN (Fig. 1A) did not provide any detectable PLA signal, revealing the specificity of PLA signal. As a positive control for primary/direct interactions, we assayed the association of CD9 with CD81, as these two tetraspanins are known to interact forming heterodimers and higher order oligomers on the cell surface [32,43,45].

Most reported lateral interactions of tetraspanins with other proteins, and particularly with integrins, occur through the variable region of their Large Extracellular Loop (LEL) domain [34,46,67]. To assess whether CD9–LFA-1 interaction is mediated through this domain, we carried out pull-down assays employing a GST-fusion protein corresponding to the LEL domain of CD9 (CD9–LEL–GST) [29,38]. The β2 subunit of endogenous LFA-1 was pulled down by CD9–LEL–GST from Brij-97 (not shown) and Triton-X100 (Fig. 3D, left panel) lysates of JY cells (and THP-1/PMA cells, not shown). As a positive control, another GST construct corresponding to the LEL domain of CD81, a tetraspanin closely related to CD9, also pulled-down the β2 integrin subunit, as previously reported [69]. In contrast, the GST-LEL construct of another tetraspanin, CD63, (CD63-LEL-GST) did not pull-down the β2 integrin subunit, reflecting the specificity of these LFA-1/tetraspanin interactions. Furthermore, the CD9–GST–LEL fusion protein selectively recovered both the β2 and the αL subunits of LFA-1 from a lysate of biotin-labeled JY cells, indicating that on these cells LFA-1 is a major surface protein that is selectively engaged in specific interactions with the LEL domain of CD9 (Fig. 3D, right panel).

3.2. CD9 regulates the adhesive function of integrin LFA-1

We decided to explore whether CD9 could regulate the adhesive function of LFA-1. For this goal, we first assessed the effects of several CD9-specific mAbs (VJ1/20, PAINS-10 and PAINS-13), which exert an agonist-like action on CD9 [29,31,32,51], on LFA-1-mediated leukocyte adhesion. Treatment of THP-1/PMA cells with the three different anti-CD9 mAbs inhibited significantly their adhesion to immobilized ligand ICAM-1 (Fig. 4A, left panel). The LFA-1-dependence of this assay was confirmed by the nearly complete inhibition of adhesion with the blocking anti-β2 mAb Lia3/2 and by the important stimulation of adhesion with the β2-activating mAb Kim185. Similar results were also obtained with B lymphoblastic JY cells, which do not express β1 integrin (Fig. 4B).

In contrast to freshly isolated resting human lymphocytes, which express very little CD9 on their surface [5,70], PHA/IL-2-activated lymphocytes ("lymphoblasts") express abundantly the integrin LFA-1 as well as variable (from donor to donor) though consistently detectable levels of CD9 on their surface, together with modest $\alpha_M\beta_2$ and negligible $\alpha_X\beta_2$ integrin expression (Fig. 4C). Using these primary human lymphoblasts in static adhesion assays on ligand ICAM-1, we observed essentially the same regulatory effects of CD9-specific mAbs on the adhesive activity of LFA-1 (Fig. 4D), indicating that CD9 exerts inhibitory effects on LFA-1-mediated adhesion.

Interaction of integrin LFA-1 with specific ligands is a crucial step in many leukocyte intercellular interactions and particularly in the cytotoxic lymphocyte-mediated killing of target cells [2,11,24,25,40]. Interestingly, the observed inhibitory effect exerted by anti-CD9 mAbs (VJ1/20, PAINS-10 and PAINS-13) on LFA-1 was also reflected in LAK (lymphokine-activated killer cells)-mediated killing of target Daudi

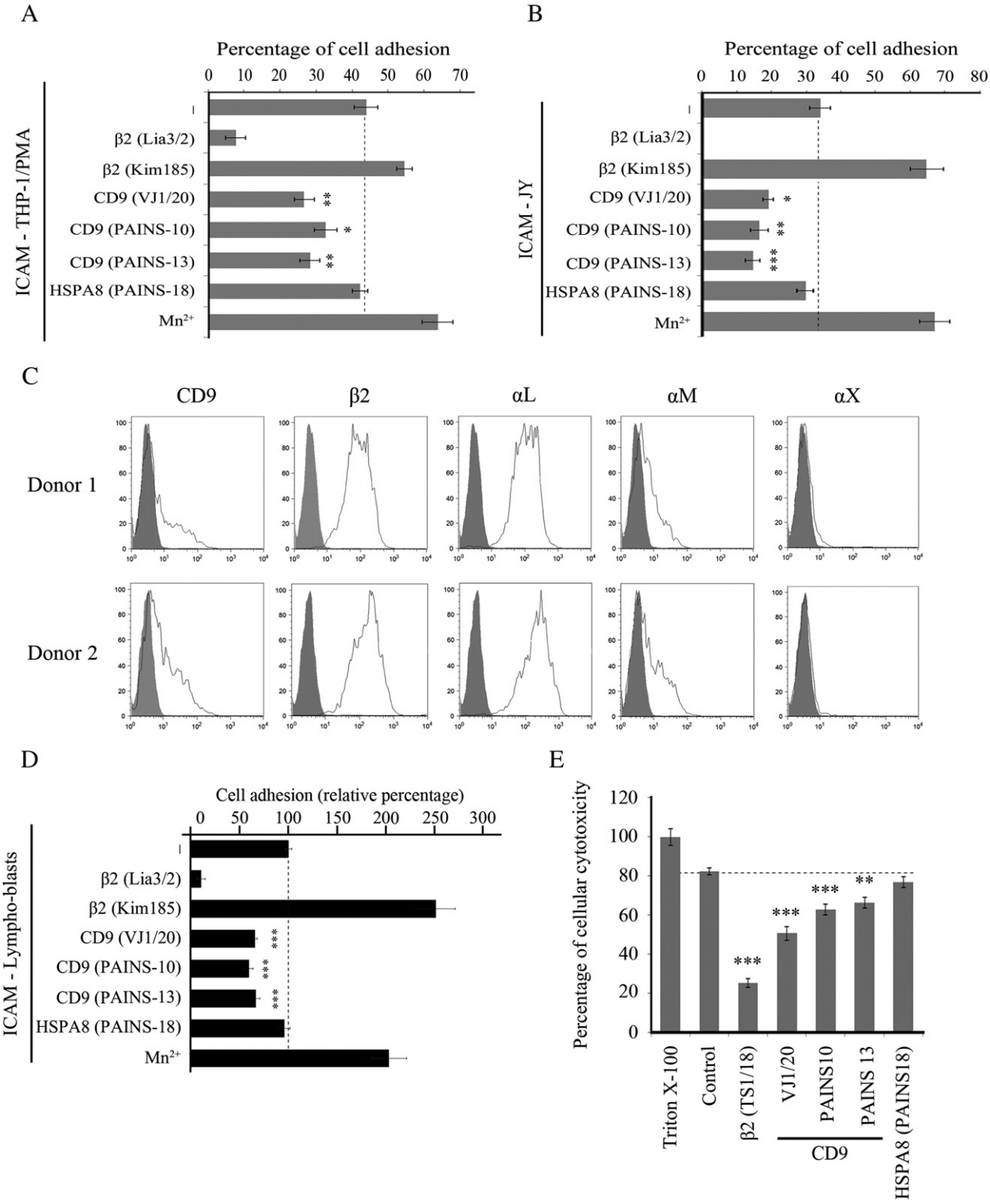

Fig. 4. Anti-CD9 mAbs inhibit LFA-1 adhesion and LAK cytotoxicity. A) THP-1/PMA cells were loaded with the fluorescent probe BCECF-AM (Sigma) and then allowed to adhere to ICAM-1-Fc-coated wells (6 μg/ml) for 20 min at 37 °C in the presence of the indicated mAbs (20 μg/ml). Data represent the percentage of adherent cells (mean ± SEM of four experiments, each performed in triplicates) that remains in the wells after washing non-adherent cells. B) JY B lymphocytic cells, loaded with the fluorescent BCECF-AM probe, were seeded in 96-well plates pre-coated with ICAM-1-Fc (12 μg/ml) and incubated for 20 min at 37 °C with the corresponding mAbs (20 μg/ml) specified. The bars-graph represents the percentage of adhesion (mean ± SEM) of 3 different experiments, performed in triplicates. C) Flow cytometric analysis of CD9 (mAb VJ1/20), β2 (mAb TS1/18), αL (mAb TP1/40), αM (mAb Bear-1) and αX (mAb HC1/1) surface molecules on human T-lymphoblasts from two different donors. D) Adhesion of T-lymphoblasts to plastic-immobilized ICAM-1-Fc (6 μg/ml). Cells were allowed to adhere for 20 min in the presence of the specified mAbs (20 μg/ml). Data shown correspond to the percentages of adherent cells (mean ± SEM of four experiments) relative to 100% cell adhesion (dotted line) considered in the absence of antibody treatment. E) LAK cytotoxic cells were pre-treated with control anti-HSPA8 mAb (PAINS-18), anti-CD9 antibodies (VJ1/20, PAINS-10 and PAINS-13) or the inhibitory anti-β2 antibody TS1/18 and their cytotoxicity was analyzed by incubating them with Daudi target cells at a 10:1 (effector:target) ratio. Cytotoxicity was determined from the amount of LDH released to the medium. The data show the percentage of cytotoxicity (mean ± SEM) of three different experiments performed in triplicates. *$p < 0.05$, **$p < 0.01$ and ***$p < 0.001$.

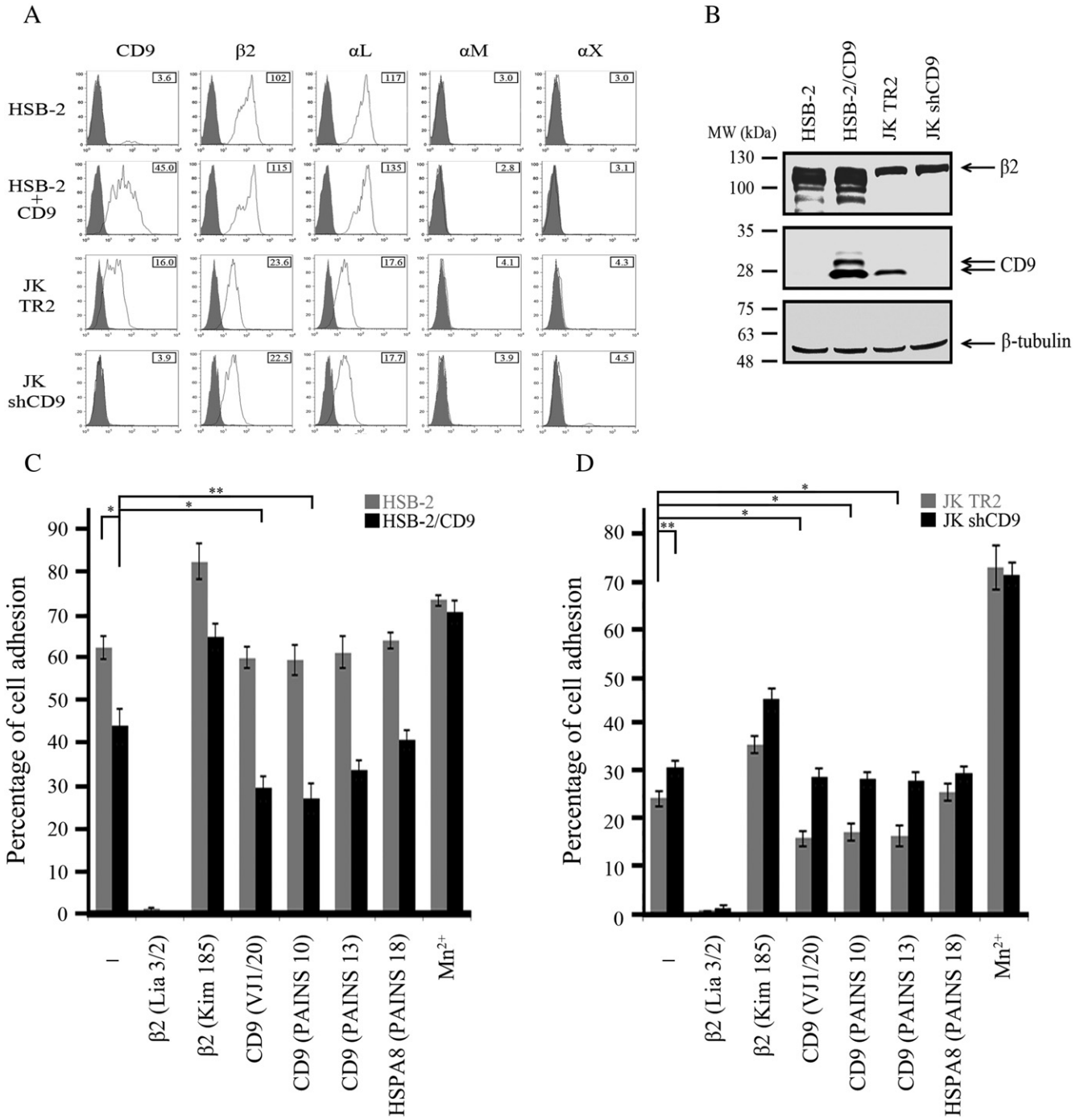

Fig. 5. Ectopic expression or silencing of CD9 regulates LFA-1 mediated adhesion. A) and B) ectopic neoexpression of CD9 in HSB-2 cells was achieved by stable transfection with the pcDNA3-CD9 (HSB-2/CD9) plasmid and CD9 knock-down in Jurkat cells was achieved by retroviral transduction with CD9-specific shRNA (JK shCD9). Jurkat cells transduced with an empty shRNA vector (JK TR2) were used as control. The neoexpression or silencing of CD9 in these cells was confirmed by flow cytometric analysis (A) and western blotting (B). C) After loading cells with BCECF-AM, HSB-2 (left panel) or Jurkat (right panel) cells were allowed to adhere for 60 min to immobilized ICAM-1-Fc (12 μg/ml), in the presence or absence of the indicated mAbs (20 μg/ml). The graphic shows the percentage of cell adhesion (mean ± SEM) of three independent experiments, each performed in triplicates. $^{*}p < 0.05$ and $^{**}p < 0.01$.

Fig. 6. CD9 regulation of LFA-1-mediated adhesion does not involve alteration of integrin affinity. A) Flow cytometric analysis of epitope m24 expression induced by Mn^{2+} (at 10, 20, 40, 100 and 400 μM) relative to its basal expression in Ca^{2+}/Mg^{2+} (0.5 mM and 1 mM, respectively) on the surface of HSB-2 (dark blue solid line), HSB-2/CD9 (light blue dotted line), JK TR2 (red dotted line) and JK shCD9 (brown solid line) cells. B) and C) JK TR2 (red bars) and JK shCD9 (brown bars) (B) or HSB-2 (dark blue bars) and HSB-2/CD9 (light blue bars) (C) cells were loaded with BCECF-AM. Then cells were treated with different Mn^{2+} concentrations and allowed to adhere for 45 min to immobilized ICAM-1-Fc (12 μg/ml), in the presence or absence of the indicated mAbs (20 μg/ml). Each bar panel shows the percentages of adherent cells (mean ± SEM of three experiments) for each Mn^{2+} concentration, and data corresponding to these different Mn^{2+} concentrations are plotted in the right panel. $^{*}p < 0.05$, $^{**}p < 0.01$ and $^{***}p < 0.001$.

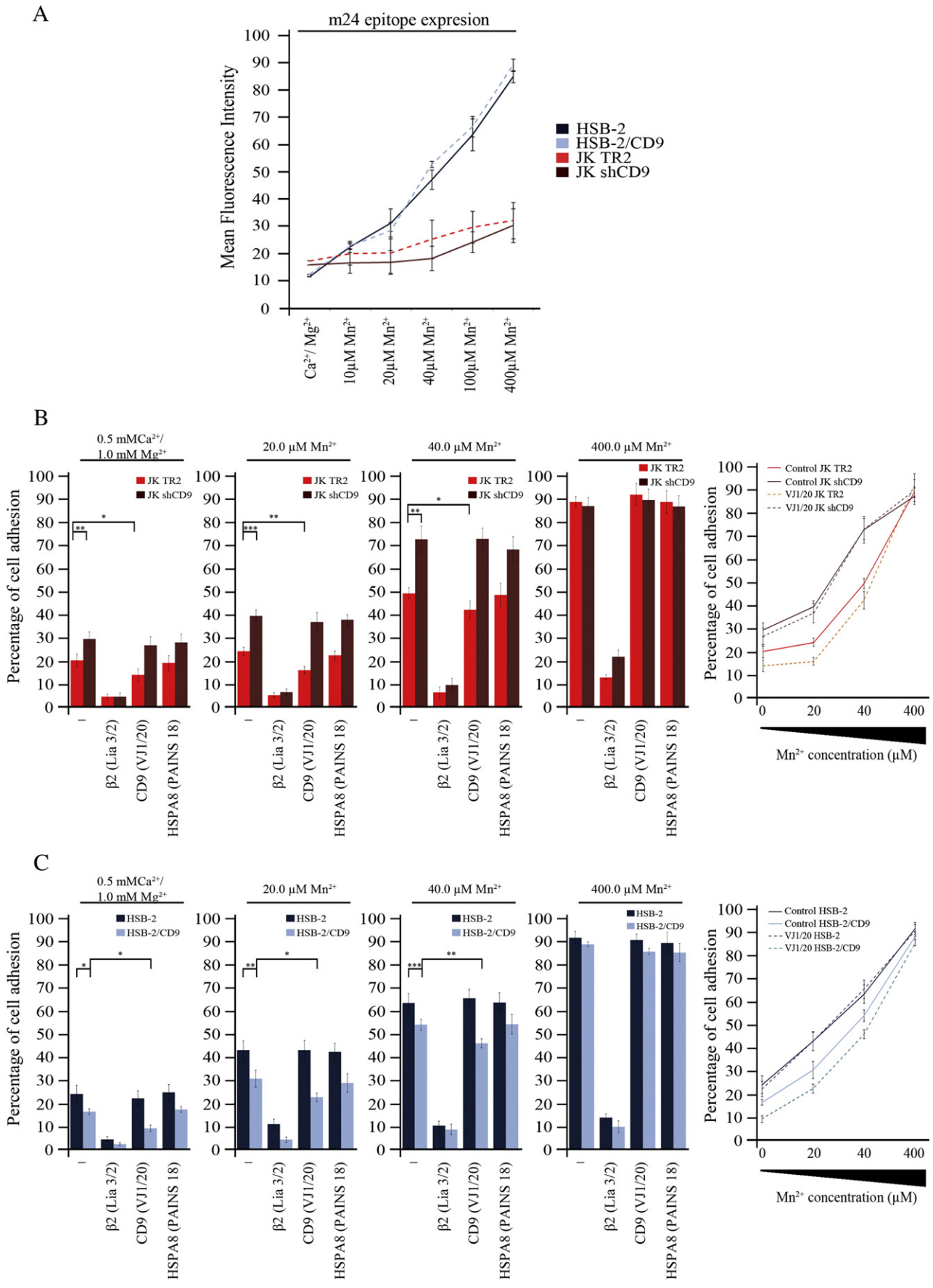
A
m24 epitope expresion
Mean Fluorescence Intensity
HSB-2
HSB-2/CD9
JK TR2
JK shCD9
Ca2+/ Mg2+
10μM Mn2+
20μM Mn2+
40μM Mn2+
100μM Mn2+
400μM Mn2+
B
0.5 mMCa2+/ 1.0 mM Mg2+
20.0 μM Mn2+
40.0 μM Mn2+
400.0 μM Mn2+
Percentage of cell adhesion
JK TR2
JK shCD9
–
β2 (Lia 3/2)
CD9 (VJ1/20)
HSPA8 (PAINS 18)
Control JK TR2
Control JK shCD9
VJ1/20 JK TR2
VJ1/20 JK shCD9
Mn2+ concentration (μM)
C
HSB-2
HSB-2/CD9
Control HSB-2
Control HSB-2/CD9
VJ1/20 HSB-2
VJ1/20 HSB-2/CD9

cells (Fig. 4E). The allosterically inhibiting anti-CD18 mAb TS1/18 [57] was used as a blocking control. Taken together, these results confirm that mAbs with agonist-like effect on CD9 regulate negatively the adhesive function of LFA-1.

We next wanted to address whether changes in the expression levels of CD9 could also regulate LFA-1 adhesiveness, either by ectopically expressing this tetraspanin in the CD9-deficient HSB-2 T lymphoblastic cell line or, conversely, by suppressing CD9 expression using shRNA interference in Jurkat T cells (Fig. 5A and B). Ectopic expression of CD9 in HSB-2 cells reduced significantly LFA-1-mediated adhesion to immobilized ligand ICAM-1 (Fig. 5C), whereas silencing CD9 in Jurkat cells enhanced LFA-1-mediated adhesion to ICAM-1 (Fig. 5D). Interestingly, incubation of HSB-2/CD9 and Jurkat T cells with the anti-CD9 mAbs VJ1/20, PAINS-10 and PAINS-13, further reduced LFA-1-mediated adhesion to ICAM-1, confirming the agonist-like effect of these mAbs on CD9 function.

3.3. CD9-mediated regulation of LFA-1 adhesion does not involve changes in integrin affinity but alters its clustering

Integrin adhesive capacity is mainly regulated by two different mechanisms involving either, alterations in the conformation of individual integrin molecules that are reflected by affinity changes, or modifications in the aggregation of integrin molecules which affect the valency of their interactions with ligand. To investigate which of these mechanisms is involved in the observed CD9-mediated inhibition of LFA-1 adhesive function, we first analyzed the induction of expression of the m24 epitope by divalent cation Mn^{2+}, which reports the high affinity conformation of LFA-1. As shown in Fig. 6A, expression of m24 epitope was similarly induced by Mn^{2+} (over the 10–400 μM concentration range) on cells expressing CD9 (HSB-2/CD9 and JK TR2 cells) and on their respective counterparts lacking CD9 (HSB-2 and JK shCD9), clearly indicating that the presence of this tetraspanin does not interfere with the affinity state of LFA-1. As expected, Mn^{2+} induced LFA-1-mediated adhesion of JK (Fig. 6B) and HSB-2 (Fig. 6C) T cells in a concentration-dependent manner over a 20–400 μM range. Interestingly, the differences in static cell adhesion between cells lacking CD9 and their CD9-expressing counterparts disappeared at the highest (400 μM) Mn^{2+} concentration. The inhibitory effect of anti-CD9 mAb VJ1/20 was also abrogated at 400 μM Mn^{2+}. These results show that CD9 does not affect LFA-1 adhesive function when cell adhesion is mediated by integrin molecules in the high affinity state (i.e. at high Mn^{2+} concentration).

However, when T cell adhesion was promoted with phorbol ester PMA (at 50 and 200 ng/ml), which induces the intermediate affinity state of LFA-1 as well as ligand-dependent clustering of this integrin, CD9-caused inhibition of static adhesion was clearly observed even at the highest PMA dose (200 ng/ml) (Fig. 7A and B), suggesting that CD9 effect was somehow related to the aggregation/clustering of LFA-1. It is worth indicating that these CD9-caused inhibitory effects on adhesion are still maintained at higher concentrations of PMA (400 ng/ml) (data not shown), although cell viability under these conditions begins to be compromised. Importantly, these differences in PMA-induced LFA-mediated cell adhesion to ICAM-1 between T cells expressing or lacking CD9 were also consistently observed under flow conditions, therefore highlighting the relevance of CD9-mediated regulation of LFA-1 function under conditions that resemble a more physiological setting (Fig. 7C).

To analyze in more detail the implication of CD9 in the organization of LFA-1 molecules, we first quantitated the number and size of LFA-1 clusters on the adhesive surface of PMA-stimulated T cells either expressing (JK TR2) or lacking CD9 (JK shCD9). As shown in Fig. 8A (upper panel), the number of PMA-induced LFA-1 clusters detected by confocal microscopy on the cellular adhesive surface in contact with immobilized ligand ICAM-1 was significantly higher on Jurkat T cells expressing CD9 than on their CD9-silenced counterparts. Interestingly, although fewer LFA-1 clusters were observed on cells lacking CD9 expression, their size was bigger than on CD9-expressing cells. Likewise, the presence of CD9 induced the organization of LFA-1 molecules into an increased number of smaller clusters in PMA-stimulated monocytic U937 cells adhering onto ICAM-1 (Fig. 8A, lower panel). These results were corroborated by TIRF microscopy, which recognizes with high resolution and high signal-to-noise ratio the organization of cell surface molecules located specifically in the area of contact with the substrate (ICAM-1). Quantitation of fluorescence from TIRF microscopy images shows that CD9-expressing T cells (JK TR2) display an increased number of clusters but of a smaller size as well as a significant proportion of LFA-1 molecules with a dispersed/unclustered appearance, compared to their CD9-lacking (JK shCD9) cell counterparts (Fig. 8B).

As a complementary biochemical approach to get further insight on how CD9 affects the organization of LFA-1 molecules on the leukocyte surface, the differential resistance of LFA-1 molecules to extraction with increasing concentrations of detergent Triton X-100 (ranging from 0.02 to 1%) in Jurkat cells expressing (JK TR2) or lacking CD9 (JK shCD9) was analyzed. As shown in Fig. 8C, LFA-1 molecules were much more easily extracted when CD9 is expressed on the cell surface, as would be expected from the increased proportion of LFA-1 found in a dispersed/unclustered form and organized in smaller clusters.

Collectively, the confocal and TIRF microscopy data together with the biochemical extraction results show that CD9 affects the organization of LFA-1 molecules into clusters, as evidenced by the differences in the number and size of LFA-1 aggregates on the cell surface as well as by their resistance to detergent extraction.

4. Discussion

We report here that the β2 integrin LFA-1 associates with CD9 in different types of leukocytes, including T (Jurkat) and B (JY) lymphocytic cell lines, and PMA-differentiated THP-1 macrophage-like cells.

The CD9/LFA-1 association was evidenced by co-localization, *in situ* Proximity Ligation Assays (PLA), as well as biochemical studies based on co-immunoprecipitation, chemical cross-linking and pull-down assays. These interactions resist stringent cell solubilization conditions (i.e. 1% Triton X-100) in co-immunoprecipitation and pull-down experiments which, together with chemical cross-linking and PLA data, collectively support the direct nature of the interaction between CD9 and LFA-1. Both co-localization and PLA signal were particularly evident at the cell–cell contact regions of THP-1 cell aggregates formed during their PMA-induced differentiation process, which are areas enriched in LFA-1 molecules actively engaged in interactions with ICAM-1 ligand expressed on opposing cells, suggesting that the association of CD9 with LFA-1 might be important in the regulation of LFA-1 adhesive function. Tetraspanin–integrin interactions seem to be consistently mediated through the variable region of the LEL domain of tetraspanins [8,20,35,79]; in this regard our pull-down experiments with a recombinant construct corresponding to the CD9 LEL-domain indicate that the

Fig. 7. CD9 regulates PMA-induced LFA-1 adhesion through an increment in integrin clustering. A) and B) prior to adhesion, JK TR2 and JK shCD9 (red and brown bars, respectively) (A) or HSB-2 and HSB-2/CD9 (dark and light blue bars, respectively) (B) cells were treated 2 h at 37 °C with different concentrations of PMA (0, 50 or 200 ng/ml). Then cells were loaded with the fluorescent probe BCECF-AM and allowed to adhere to plastic-immobilized ICAM-1-Fc (12 μg/ml) for 45 min at 37 °C in the presence or absence of the indicated mAbs (20 μg/ml). Data represent the percentages of adherent cells (mean ± SEM of three experiments), and data corresponding to these different PMA concentrations are plotted in the right panel. C) Adhesion of PMA-stimulated JK TR2 and JK shCD9 cells to ICAM-1 under shear flow conditions. Left panel contains a representative image showing the cells that remain adhered for each different flow rate, and the right panel graph shows the calculated ratios of adherent cells from 9 different microscopic fields for each flow rate condition. *$p < 0.05$, **$p < 0.01$ and ***$p < 0.001$. Scale bars = 30 μm.

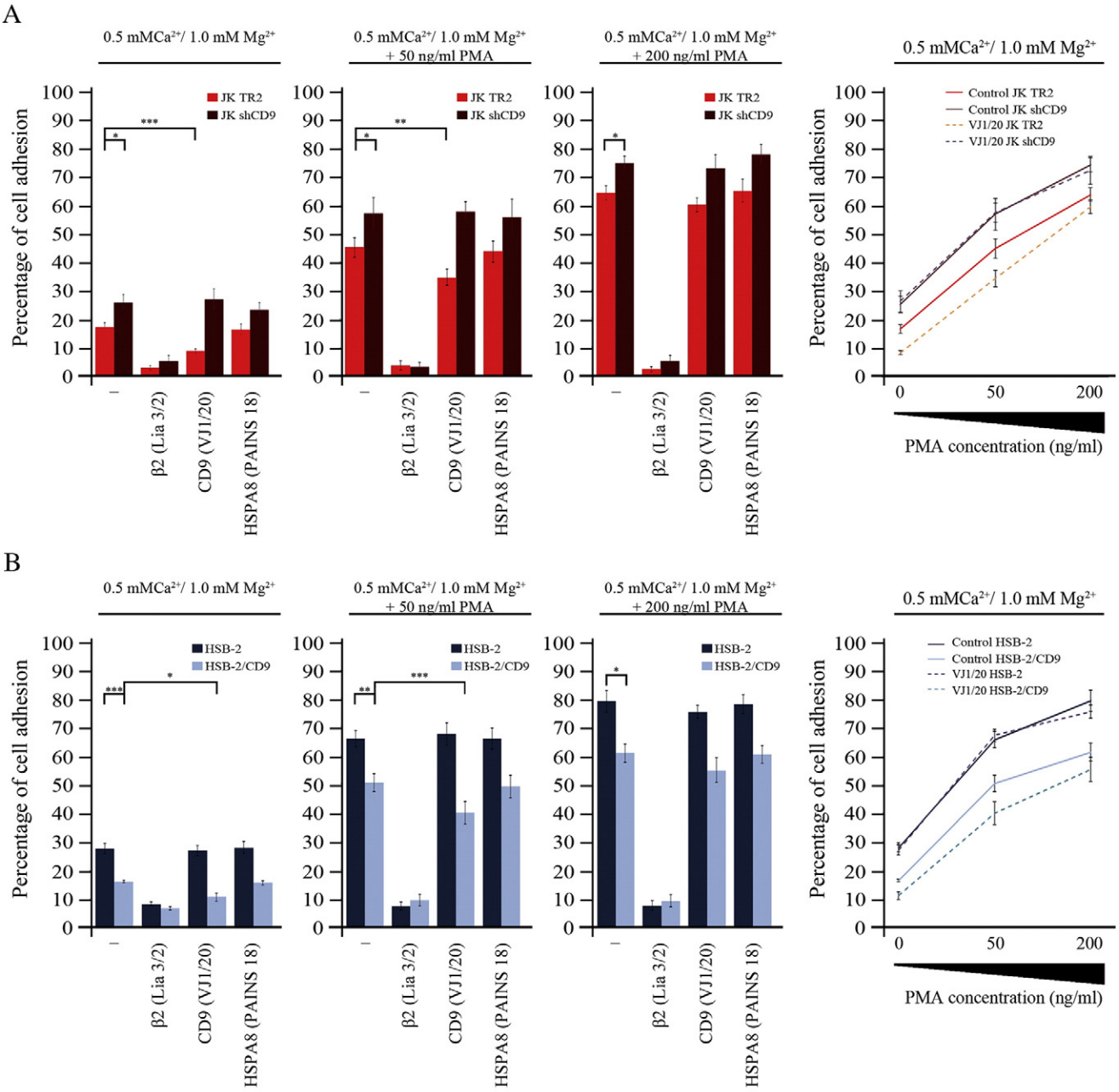
A
0.5 mMCa2+/ 1.0 mM Mg2+
0.5 mMCa2+/ 1.0 mM Mg2+ + 50 ng/ml PMA
0.5 mMCa2+/ 1.0 mM Mg2+ + 200 ng/ml PMA
JK TR2
JK shCD9
Percentage of cell adhesion
–
β2 (Lia 3/2)
CD9 (VJ1/20)
HSPA8 (PAINS 18)
Control JK TR2
Control JK shCD9
VJ1/20 JK TR2
VJ1/20 JK shCD9
PMA concentration (ng/ml)
B
HSB-2
HSB-2/CD9
Control HSB-2
Control HSB-2/CD9
VJ1/20 HSB-2
VJ1/20 HSB-2/CD9

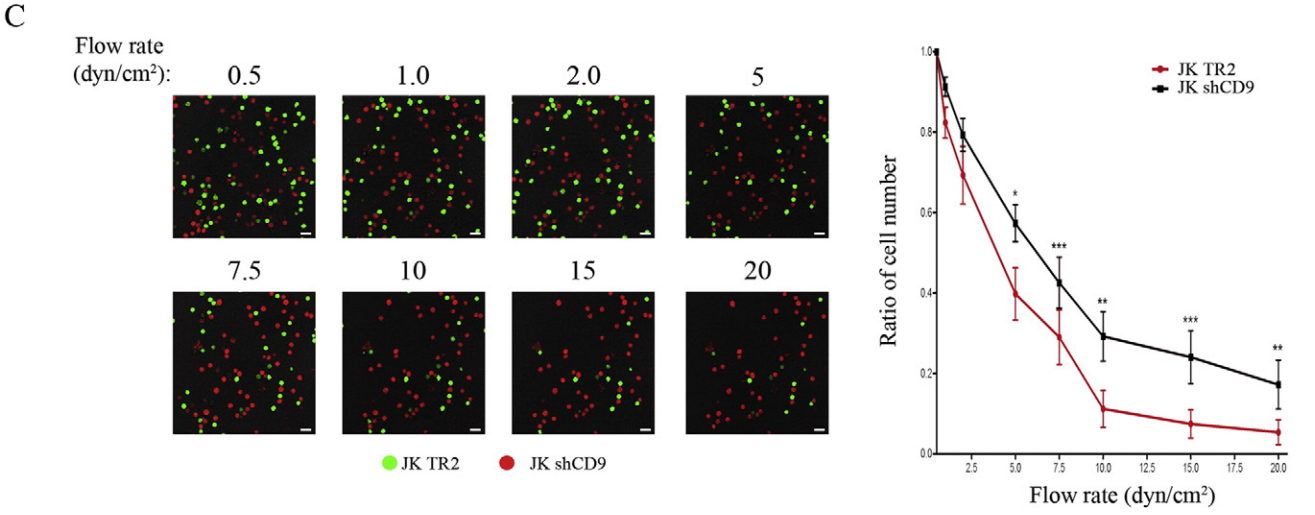
C
Flow rate (dyn/cm2):
0.5
1.0
2.0
5
7.5
10
15
20
JK TR2
JK shCD9
Ratio of cell number
Flow rate (dyn/cm2)

interaction between β2 integrin and CD9 is also mediated by this domain.

After demonstrating the existence of CD9–LFA-1 complexes in different types of leukocytes we next explored whether CD9 exerted any functional effects on the adhesive capacity of LFA-1. For this purpose, we have made use of three different anti-CD9 mAbs (VJ1/20, PAINS-10 and PAINS-13) considered to exert, at the cellular level, an agonist-like action on the basis that in different cellular systems the functional effects caused by treating $CD9^+$ cells with these antibodies are similar to those derived from the neo- or over-expression of CD9, but opposite to those observed after silencing this tetraspanin [29,32,51]. The use of these three anti-CD9 mAbs, as well as ectopic expression of CD9 in HSB-2 T cells or silencing the endogenous CD9 expression in Jurkat T cells using specific shRNAs, collectively show that CD9 exerts a negative regulatory role on LFA-1-mediated leukocyte adhesion. Consistently with the CD9 inhibitory effect on adhesion, LAK-cellular cytotoxicity against target cells, which is largely dependent on LFA-1-mediated intercellular adhesion, was also inhibited by these anti-CD9 mAbs. Engagement of tetraspanins CD81 or CD82 with specific mAbs or overexpression of these molecules on T cells has been reported to upregulate the adhesive and signaling capacities of the integrin LFA-1 [62,75], whereas for the tetraspanin CD9 we report here the opposite: a clear inhibitory effect on LFA-1-mediated cellular adhesion and *in vitro* cellular cytotoxicity. One possibility is that the different functional effects of distinct tetraspanins on LFA-1 adhesive function might depend on the specific cellular system under study or the specific ligand employed (ICAM-3 employed in some of these previous reports *versus* ICAM-1 employed here), or alternatively CD9 may exert specific functional effects on LFA-1.

Integrin adhesive capacity can be regulated essentially by mechanisms involving either alterations in the affinity of individual integrin molecules or changes in their aggregation/clustering on the cell surface which regulate the valency of their interactions with ligand. As reported by the expression of the m24 epitope, the high affinity conformation of LFA-1 induced by Mn^{2+} was not altered by ectopic expression or silencing of CD9; accordingly, no differences were observed in LFA-1-mediated adhesion stimulated by 400 μM Mn^{2+} between cells expressing or lacking CD9. In contrast, it is interesting that at lower Mn^{2+} concentrations (20 and 40 μM), at which presumably only a proportion of total LFA-1 molecules are in the high affinity conformation, differences in adhesion between cells expressing or lacking CD9 could be observed. Moreover, the differences between cells expressing and lacking CD9 were also consistently observed when cell adhesion was promoted with PMA, which induces the intermediate affinity state of LFA-1 as well as ligand-dependent clustering of this integrin. All these results clearly indicated that the effect of CD9 on LFA-1-mediated adhesion was mainly related to the aggregation/clustering state of this integrin and not to changes in its affinity. Indeed, confocal and TIRF microscopy analyses of PMA-induced LFA-1 clustering specifically at the adhesive cellular surface in contact with immobilized ligand ICAM-1 showed that in leukocytic cells expressing CD9 an increased number of clusters but with a smaller size could be detected in comparison with their CD9-lacking cell counterparts. TIRF microscopy images also revealed that in T cells expressing CD9 a significant proportion of LFA-1 molecules showed a dispersed/unclustered appearance, which might correspond to the nanoclusters of LFA-1 that have been characterized by other higher resolution microscopy techniques. In this regard, through the use of NSOM (near-field scanning optical microscopy) and SDT (single dye tracking) super-resolution optical techniques, it has been recently reported that LFA-1 is preorganized in nanoclusters in "hotspot" regions of the leukocyte membrane. Ligand binding favors the lateral mobility and growth of LFA-1 clusters through coalescence of individual nanoclusters to form microclusters, in a process that also critically depends on transient cytoskeleton anchorage, which in turn mediate efficient stable leukocyte adhesion under shear flow [3,74]. Our findings are therefore compatible with these observations, and we can speculate that CD9 might have an important role in regulating these transitions among the different states of LFA-1 organization into distinct types of differently-sized clusters as well as the anchorage to the actin cytoskeleton.

Interestingly, we have observed that the β1 integrin-mediated adhesion of leukocytes to the extracellular matrix protein fibronectin was enhanced by anti-CD9 mAbs or following ectopic expression of this tetraspanin (data not shown), which concurs with our previous data with colorectal carcinoma cells [51]. Therefore, CD9 seems to have a dual functional regulatory role on leukocyte adhesion mechanisms by increasing β1 adhesion to fibronectin but down-regulating LFA-1-mediated adhesion. Reciprocal control of the activity of members of distinct subfamilies of integrins co-expressed on the same cell has been previously described. For instance, in some leukemic T cell lines functionally active integrin α4β1 occurs only when LFA-1 is either not expressed or inactive [73], whereas in human erythroleukemic K562 cells transfected with integrin αvβ3, ligation of the β3 integrin subunit inhibits the phagocytic function of endogenously expressed α5β1 integrin [12,13]. Similarly, in human T lymphoblasts induction of activation of LFA-1 resulted in decreased adhesion through α4β1 and α5β1 integrins, rendering cells with a less adhesive and more migratory phenotype [52]. However, the underlying mechanisms for this type of regulation are still unclear. Association with cytoskeleton is essential for integrin activation and adhesion. Interestingly, actin cytoskeleton seems to play a differential role in the control of β1 and β2 integrin function. In this regard, in resting leukocytes LFA-1 molecules are maintained in an inactive low-avidity state through association with actin microfilaments and release from these cytoskeletal constraints, caused by drugs such as cytochalasin D or latrunculin B, increases their lateral diffusion which is accompanied by enhanced clustering and avidity and augmented LFA-1-mediated leukocyte adhesion to ICAM-expressing cells [44,71]. In contrast, most β1 integrins (with the notable exception of α4β1 interaction with VCAM-1) mediate a more stable type of cell adhesion to extracellular matrix proteins such as fibronectin, collagen and laminin, and for this purpose seem to require firmer links with cytoskeletal components [10,22,59]. Several tetraspanins, including CD81 and CD9, are linked to actin microfilaments through ERM (Ezrin–Radixin–Moesin) proteins, either directly or through tetraspanin-associated partners EWI-2 and EWI-F [56]. The fact that CD9 may modulate in an opposite manner the adhesive function of β2 and β1 integrins points to CD9-centered TEMs as crucial players in this balanced regulation. An attractive possibility is that, by reinforcing the integrin-cytoskeletal links, CD9 may restrict the membrane lateral diffusion of LFA-1 molecules resulting in inhibition of its adhesive function, while at the same time, stabilizing β1 integrins with concomitant adhesion enhancement to matrix components. Further research will be required to properly address this attractive hypothesis.

The model depicted in Fig. 9 summarizes the main findings of this report. State "1" in the model is characterized by expression of dispersed

Fig. 8. CD9 regulates the distribution of LFA-1 molecules into clusters. A) Confocal microscopy images of immunofluorescence-stained β2 integrin clustering at the adhesive surface in contact with ligand ICAM-1-Fc of PMA-stimulated JK TR2, JK shCD9, U937/pcDNA3 and U937/CD9 cells. Representative confocal images are shown on the left panels and quantitation of the number and size (mean area) of clusters/cell corresponding to ten individual cells are shown on the right panels. *$p < 0.05$, **$p < 0.01$ and ***$p < 0.001$. Scale bars = 5 μm. B) TIRF microscopy images of β2 integrin clustering at the adhesive surface in contact with ligand ICAM-1-Fc of PMA-stimulated JK TR2, JK shCD9. Five representative images are shown for each cell type on the left panel and quantitation of the number and size of clusters/cell corresponding to 15 individual cells are shown on the right panels. ***$p < 0.001$. Scale bars = 5 μm. C) Differential resistance of LFA-1 molecules to extraction with increasing concentrations of detergent Triton X-100 (0.02/0.05/0.1/0.5%) from PMA-stimulated Jurkat cells either expressing (JK TR2) or lacking CD9 (JK shCD9), adhered to ICAM-1-Fc. Extracted LFA-1 was detected by immunoblotting with the anti-β2 mAb MEM48, and quantitated relative to β-actin content.

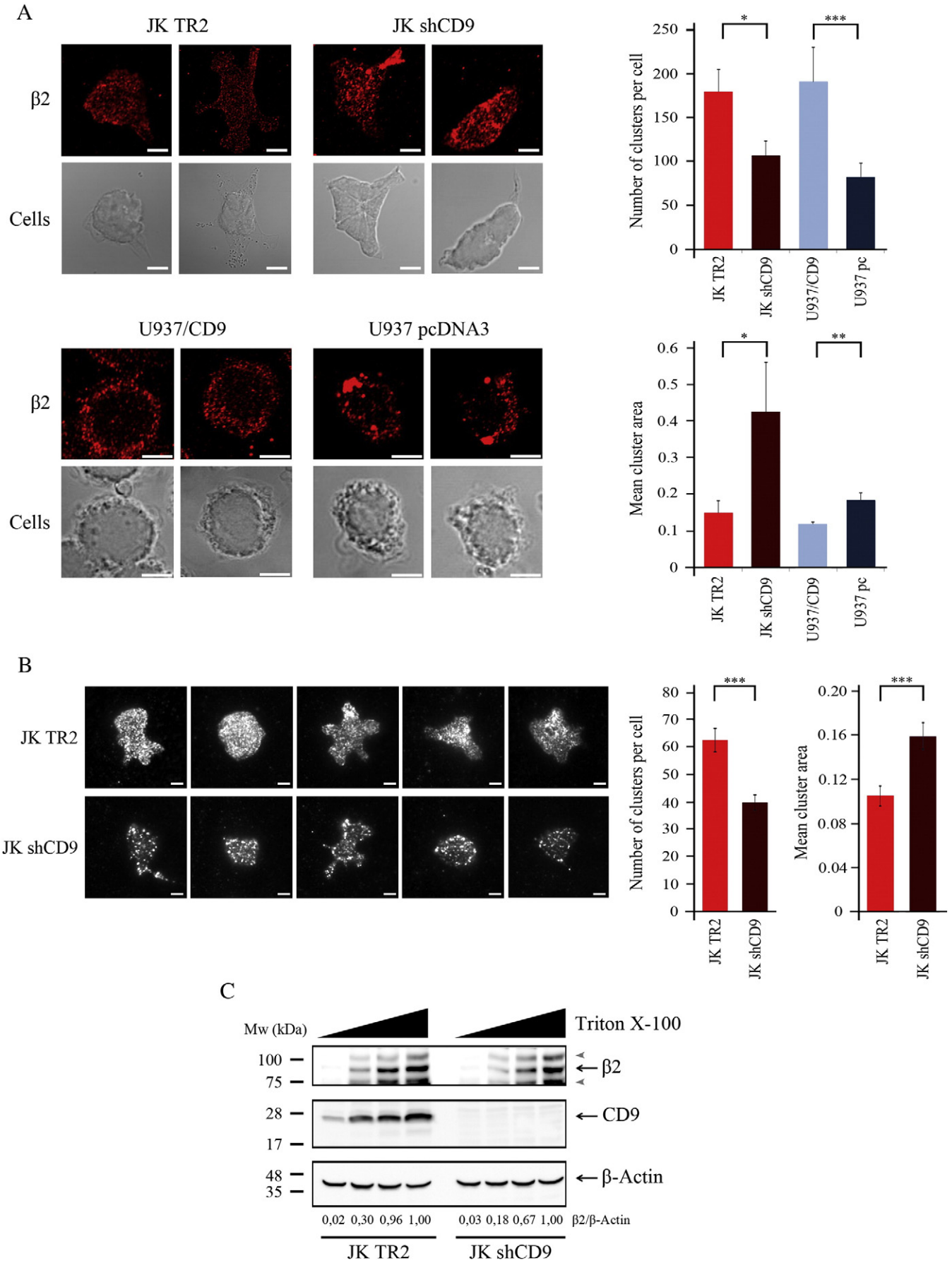
A
JK TR2
JK shCD9
β2
Cells
U937/CD9
U937 pcDNA3
β2
Cells
Number of clusters per cell
250
200
150
100
50
0
*
***
JK TR2
JK shCD9
U937/CD9
U937 pc
Mean cluster area
0.6
0.5
0.4
0.3
0.2
0.1
0
*
**
JK TR2
JK shCD9
U937/CD9
U937 pc
B
JK TR2
JK shCD9
Number of clusters per cell
80
70
60
50
40
30
20
10
0
***
JK TR2
JK shCD9
Mean cluster area
0.20
0.16
0.12
0.08
0.04
0
***
JK TR2
JK shCD9
C
Mw (kDa)
Triton X-100
100
75
β2
28
17
CD9
48
35
β-Actin
0,02 0,30 0,96 1,00
0,03 0,18 0,67 1,00
β2/β-Actin
JK TR2
JK shCD9

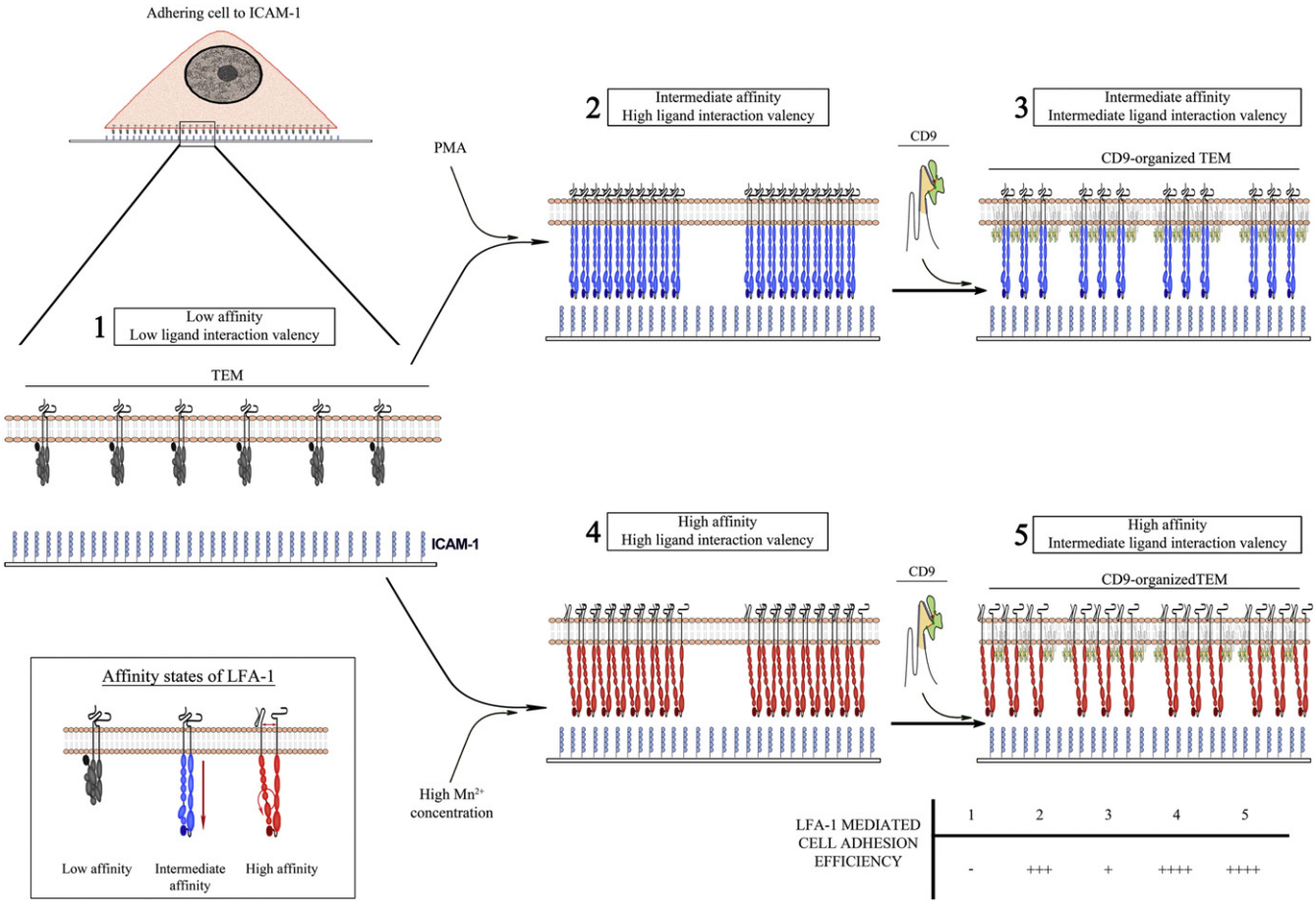

Fig. 9. Hypothetical model which summarizes the regulation by CD9 of the different LFA-1 functional states, as described in the Discussion.

and inactive/bent form of LFA-1 (Low-valency/Low-affinity) and by the absence/very low expression of CD9, as occurs physiologically in most resting/non-stimulated lymphocytes [5,70]. Conversion from state "1" into a High-valency/Intermediate-affinity state ("2") is characterized by aggregation of integrin molecules into large clusters and the acquisition of intermediate affinity conformation, both induced by phorbol ester PMA. Within the context of TEMs, augmented CD9 function induced by its ectopic neoexpression (or by the use of agonist-like mAbs to this tetraspanin, not shown in the model), alters the organization of LFA-1 molecules at the cell adhesion surface, as evidenced by an increase in "dispersed" LFA-1 molecules and in the number of clusters with a reduced size, defining an Intermediate-valency/Intermediate-affinity state ("3") characterized by diminished adhesive efficiency to ligand ICAM-1 relative to state "2". On the other hand, state "4" is induced by high concentration of Mn^{2+} and is characterized by clustering of LFA-1 molecules in a high affinity conformation (High-valency/High-affinity state); in this case, transition from state "4" into "5", caused by the ectopic expression of CD9 (or by the use of agonist-like mAbs to this tetraspanin, not shown in the model), is not accompanied by a down-modulation of the adhesive efficiency because, although probably some reduction in the ligand-interaction valency occurs, this effect is not potent enough to decrease cell adhesion when mediated by a majority of LFA-1 molecules in the high affinity conformation. The inhibitory effects on LFA-1-mediated cell adhesion (observed in transitions "2"→"3") could place CD9 as a novel target for therapeutic intervention aimed at reducing the activity of LFA-1, which would be potentially beneficial in a number of inflammatory disorders.

5. Conclusions

Our data demonstrate that the tetraspanin CD9 associates with integrin LFA-1 in different types of leukocytes, and through these interactions, CD9 exerts inhibitory effects on LFA-1 adhesive function and leukocyte cytotoxic activity. The mechanism responsible for this negative modulation exerted by CD9 does not involve changes in the affinity state of LFA-1 but relates to alterations in its state of aggregation. These data contribute to our understanding of the regulation of adhesive activity of LFA-1, an integrin that plays a pivotal role in many crucial leukocyte functions that require intercellular adhesion.

Abbreviations

BSA	bovine serum albumin
FBS	fetal bovine serum
FITC	fluorescein isothiocyanate
GST	glutathione S-transferase
ICAM-1	intercellular adhesion molecule-1
IL-2	interleukin 2
INT	2-(p-iodophenyl)-3-(p-nitrophenyl)-5-phenyltetrazolium chloride
LDH	lactate dehydrogenase
LAK	lymphokine-activated killer
LEL	large extracellular loop
mAb	monoclonal antibody
M.F.I.	mean fluorescence intensity

PBLs peripheral blood leukocytes
PBS phosphate buffered saline
PLAs proximity ligation assays
PMA phorbol myristate acetate
SDS sodium dodecyl sulfate
SDS-PAGE sodium dodecyl sulfate polyacrylamide gel electrophoresis
SEM standard error of the mean
TBS tris buffered saline
TEM tetraspanin-enriched microdomain
TIRF total internal reflection fluorescence

Supplementary data to this article can be found online at http://dx.doi.org/10.1016/j.bbamcr.2015.05.018.

Authors' contributions

RR carried out the confocal and TIRF microscopy, biochemical studies, flow cytometry, gene transfection, silencing and cell adhesion experiments. She also participated in the design of the study and performed the statistical analysis. AM performed confocal microscopy and some biochemical studies and adhesion experiments. She also participated in the design of the study. MYM carried out confocal and TIRF microscopy and biochemical experiments and participated in the interpretation of data and helped to draft the manuscript. BC performed some biochemical experiments. GM performed cell adhesion experiments. AG performed some adhesion experiments. YM participated in the flow cytometry and cell adhesion experiments. EL participated in the transfection, silencing and cell adhesion experiments and helped to draft the manuscript. PM participated in the pull-down experiments and in the interpretation of data. FSM participated in the conception and design and interpretation of data, and helped to draft the manuscript. CC conceived the study, and took responsibility for its design and coordination and wrote the manuscript.

Competing interests

The authors declare that they have no competing interests.

Transparency document

The Transparency document associated with this article can be found, in the online version.

Acknowledgements

This work was supported by grant SAF2012-34561 from the Spanish «Ministerio de Economía y Competitividad-MINECO», (to C.C.). R.R. salary has been supported by a «Profesor Ayudante» position from Departamento de Biología, Facultad de Ciencias, Universidad Autónoma de Madrid.

References

[1] P. Aller, C. Rius, F. Mata, A. Zorrilla, C. Cabanas, T. Bellon, C. Bernabeu, Camptothecin induces differentiation and stimulates the expression of differentiation-related genes in U-937 human promonocytic leukemia cells, Cancer Res. 52 (1992) 1245–1251.
[2] N. Anikeeva, K. Somersalo, T.N. Sims, V.K. Thomas, M.L. Dustin, Y. Sykulev, Distinct role of lymphocyte function-associated antigen-1 in mediating effective cytolytic activity by cytotoxic T lymphocytes, Proc. Natl. Acad. Sci. U. S. A. 102 (2005) 6437–6442.
[3] G.J. Bakker, C. Eich, J.A. Torreno-Pina, R. Diez-Ahedo, G. Perez-Samper, T.S. van Zanten, C.G. Figdor, A. Cambi, M.F. Garcia-Parajo, Lateral mobility of individual integrin nanoclusters orchestrates the onset for leukocyte adhesion, Proc. Natl. Acad. Sci. U. S. A. 109 (2012) 4869–4874.
[4] O. Barreiro, M. Yanez-Mo, M. Sala-Valdes, M.D. Gutierrez-Lopez, S. Ovalle, A. Higginbottom, P.N. Monk, C. Cabanas, F. Sanchez-Madrid, Endothelial tetraspanin microdomains regulate leukocyte firm adhesion during extravasation, Blood 105 (2005) 2852–2861.
[5] S. Barrena, J. Almeida, M. Yunta, A. Lopez, N. Fernandez-Mosteirin, M. Giralt, M. Romero, L. Perdiguer, M. Delgado, A. Orfao, et al., Aberrant expression of tetraspanin molecules in B-cell chronic lymphoproliferative disorders and its correlation with normal B-cell maturation, Leukemia 19 (2005) 1376–1383.
[6] S. Bassani, L.A. Cingolani, Tetraspanins: interactions and interplay with integrins, Int. J. Biochem. Cell Biol. 44 (2012) 703–708.
[7] F. Berditchevski, Complexes of tetraspanins with integrins: more than meets the eye, J. Cell Sci. 114 (2001) 4143–4151.
[8] F. Berditchevski, E. Gilbert, M.R. Griffiths, S. Fitter, L. Ashman, S.J. Jenner, Analysis of the CD151-alpha3beta1 integrin and CD151-tetraspanin interactions by mutagenesis, J. Biol. Chem. 276 (2001) 41165–41174.
[9] A.R. Berendt, A. McDowall, A.G. Craig, P.A. Bates, M.J. Sternberg, K. Marsh, C.I. Newbold, N. Hogg, The binding site on ICAM-1 for *Plasmodium falciparum*-infected erythrocytes overlaps, but is distinct from, the LFA-1-binding site, Cell 68 (1992) 71–81.
[10] A.L. Berrier, K.M. Yamada, Cell-matrix adhesion, J. Cell. Physiol. 213 (2007) 565–573.
[11] D. Blanchard, C. van Els, J. Borst, S. Carrel, A. Boylston, J.E. de Vries, H. Spits, The role of the T cell receptor, CD8, and LFA-1 in different stages of the cytolytic reaction mediated by alloreactive T lymphocyte clones, J. Immunol. 138 (1987) 2417–2421.
[12] S.D. Blystone, I.L. Graham, F.P. Lindberg, E.J. Brown, Integrin alpha v beta 3 differentially regulates adhesive and phagocytic functions of the fibronectin receptor alpha 5 beta 1, J. Cell Biol. 127 (1994) 1129–1137.
[13] S.D. Blystone, F.P. Lindberg, S.E. LaFlamme, E.J. Brown, Integrin beta 3 cytoplasmic tail is necessary and sufficient for regulation of alpha 5 beta 1 phagocytosis by alpha v beta 3 and integrin-associated protein, J. Cell Biol. 130 (1995) 745–754.
[14] C. Boucheix, J.Y. Perrot, M. Mirshahi, F. Giannoni, M. Billard, A. Bernadou, C. Rosenfeld, A new set of monoclonal antibodies against acute lymphoblastic leukemia, Leuk. Res. 9 (1985) 597–604.
[15] C. Cabanas, M. Mittelbrunn, F. Sanchez-Madrid, Integrin Alpha L, UCSD-Nature Molecule Pages 2008, http://dx.doi.org/10.1038/mp.a001209.01.
[16] C. Cabanas, F. Sanchez-Madrid, A. Acevedo, T. Bellon, J.M. Fernandez, V. Larraga, C. Bernabeu, Characterization of a CD11c-reactive monoclonal antibody (HC1/1) obtained by immunizing with phorbol ester differentiated U937 cells, Hybridoma 7 (1988) 167–176.
[17] M.R. Campanero, M.A. del Pozo, A.G. Arroyo, P. Sanchez-Mateos, T. Hernandez-Caselles, A. Craig, R. Pulido, F. Sanchez-Madrid, ICAM-3 interacts with LFA-1 and regulates the LFA-1/ICAM-1 cell adhesion pathway, J. Cell Biol. 123 (1993) 1007–1016.
[18] C.V. Carman, T.A. Springer, Integrin avidity regulation: are changes in affinity and conformation underemphasized? Curr. Opin. Cell Biol. 15 (2003) 547–556.
[19] C. Cluzel, F. Saltel, J. Lussi, F. Paulhe, B.A. Imhof, B. Wehrle-Haller, The mechanisms and dynamics of (alpha)v(beta)3 integrin clustering in living cells, J. Cell Biol. 171 (2005) 383–392.
[20] S. Charrin, F. le Naour, O. Silvie, P.E. Milhiet, C. Boucheix, E. Rubinstein, Lateral organization of membrane proteins: tetraspanins spin their web, Biochem. J. 420 (2009) 133–154.
[21] S. Charrin, F. Le Naour, M. Oualid, M. Billard, G. Faure, S.M. Hanash, C. Boucheix, E. Rubinstein, The major CD9 and CD81 molecular partner. Identification and characterization of the complexes, J. Biol. Chem. 276 (2001) 14329–14337.
[22] E.J. Chen, M.H. Shaffer, E.K. Williamson, Y. Huang, J.K. Burkhardt, Ezrin and moesin are required for efficient T cell adhesion and homing to lymphoid organs, PLoS ONE 8 (2013) e52368.
[23] M.S. Chen, K.S. Tung, S.A. Coonrod, Y. Takahashi, D. Bigler, A. Chang, Y. Yamashita, P.W. Kincade, J.C. Herr, J.M. White, Role of the integrin-associated protein CD9 in binding between sperm ADAM 2 and the egg integrin alpha6beta1: implications for murine fertilization, Proc. Natl. Acad. Sci. U. S. A. 96 (1999) 11830–11835.
[24] J.E. de Vries, H. Yssel, H. Spits, Interplay between the TCR/CD3 complex and CD4 or CD8 in the activation of cytotoxic T lymphocytes, Immunol. Rev. 109 (1989) 119–141.
[25] I. Dransfield, C. Cabanas, J. Barrett, N. Hogg, Interaction of leukocyte integrins with ligand is necessary but not sufficient for function, J. Cell Biol. 116 (1992) 1527–1535.
[26] I. Dransfield, C. Cabanas, A. Craig, N. Hogg, Divalent cation regulation of the function of the leukocyte integrin LFA-1, J. Cell Biol. 116 (1992) 219–226.
[27] M.L. Dustin, T.A. Springer, T-cell receptor cross-linking transiently stimulates adhesiveness through LFA-1, Nature 341 (1989) 619–624.
[28] C.G. Gahmberg, L. Valmu, A. Kotovuori, P. Kotovuori, T.J. Hilden, S. Fagerholm, C. Kantor, T. Nurminen, E. Ihanus, L. Tian, Leukocyte adhesion—an integrated molecular process at the leukocyte plasma membrane, Biosci. Rep. 19 (1999) 273–281.
[29] A. Gilsanz, L. Sanchez-Martin, M.D. Gutierrez-Lopez, S. Ovalle, Y. Machado-Pineda, R. Reyes, G.W. Swart, C.G. Figdor, E.M. Lafuente, C. Cabanas, ALCAM/CD166 adhesive function is regulated by the tetraspanin CD9, Cell. Mol. Life Sci. 70 (2013) 475–493.
[30] P. Groscurth, S. Diener, R. Stahel, L. Jost, D. Kagi, H. Hengartner, Morphologic analysis of human lymphokine-activated killer (LAK) cells, Int. J. Cancer 45 (1990) 694–704.
[31] M.D. Gutierrez-Lopez, S. Ovalle, M. Yanez-Mo, N. Sanchez-Sanchez, E. Rubinstein, N. Olmo, M.A. Lizarbe, F. Sanchez-Madrid, C. Cabanas, A functionally relevant conformational epitope on the CD9 tetraspanin depends on the association with activated beta1 integrin, J. Biol. Chem. 278 (2003) 208–218.
[32] M.D. Gutierrez-Lopez, A. Gilsanz, M. Yanez-Mo, S. Ovalle, E.M. Lafuente, C. Dominguez, P.N. Monk, I. Gonzalez-Alvaro, F. Sanchez-Madrid, C. Cabanas, The sheddase activity of ADAM17/TACE is regulated by the tetraspanin CD9, Cell. Mol. Life Sci. 68 (2011) 3275–3292.
[33] E.S. Harris, T.M. McIntyre, S.M. Prescott, G.A. Zimmerman, The leukocyte integrins, J. Biol. Chem. 275 (2000) 23409–23412.
[34] M.E. Hemler, Tetraspanin proteins mediate cellular penetration, invasion, and fusion events and define a novel type of membrane microdomain, Annu. Rev. Cell Dev. Biol. 19 (2003) 397–422.
[35] M.E. Hemler, Tetraspanin functions and associated microdomains, Nat. Rev. Mol. Cell Biol. 6 (2005) 801–811.
[36] M.E. Hemler, Tetraspanin proteins promote multiple cancer stages, Nat. Rev. Cancer 14 (2013) 49–60.

[37] A. Higginbottom, Y. Takahashi, L. Bolling, S.A. Coonrod, J.M. White, L.J. Partridge, P.N. Monk, Structural requirements for the inhibitory action of the CD9 large extracellular domain in sperm/oocyte binding and fusion, Biochem. Biophys. Res. Commun. 311 (2003) 208–214.
[38] S.H. Ho, F. Martin, A. Higginbottom, L.J. Partridge, V. Parthasarathy, G.W. Moseley, P. Lopez, C. Cheng-Mayer, P.N. Monk, Recombinant extracellular domains of tetraspanin proteins are potent inhibitors of the infection of macrophages by human immunodeficiency virus type 1, J. Virol. 80 (2006) 6487–6496.
[39] N. Hogg, I. Patzak, F. Willenbrock, The insider's guide to leukocyte integrin signalling and function, Nat. Rev. Immunol. 11 (2011) 416–426.
[40] N. Hogg, M. Laschinger, K. Giles, A. McDowall, T-cell integrins: more than just sticking points, J. Cell Sci. 116 (2003) 4695–4705.
[41] G.D. Keizer, J. Borst, C.G. Figdor, H. Spits, F. Miedema, C. Terhorst, J.E. De Vries, Biochemical and functional characteristics of the human leukocyte membrane antigen family LFA-1, Mo-1 and p150,95, Eur. J. Immunol. 15 (1985) 1142–1148.
[42] M. Kim, C.V. Carman, W. Yang, A. Salas, T.A. Springer, The primacy of affinity over clustering in regulation of adhesiveness of the integrin {alpha}L{beta}2, J. Cell Biol. 167 (2004) 1241–1253.
[43] O.V. Kovalenko, X. Yang, T.V. Kolesnikova, M.E. Hemler, Evidence for specific tetraspanin homodimers: inhibition of palmitoylation makes cysteine residues available for cross-linking, Biochem. J. 377 (2004) 407–417.
[44] D.F. Kucik, M.L. Dustin, J.M. Miller, E.J. Brown, Adhesion-activating phorbol ester increases the mobility of leukocyte integrin LFA-1 in cultured lymphocytes, J. Clin. Invest. 97 (1996) 2139–2144.
[45] F. Le Naour, M. Andre, C. Boucheix, E. Rubinstein, Membrane microdomains and proteomics: lessons from tetraspanin microdomains and comparison with lipid rafts, Proteomics 6 (2006) 6447–6454.
[46] S. Levy, T. Shoham, The tetraspanin web modulates immune-signalling complexes, Nat. Rev. Immunol. 5 (2005) 136–148.
[47] Q. Li, A. Lau, T.J. Morris, L. Guo, C.B. Fordyce, E.F. Stanley, A syntaxin 1, Galpha(o), and N-type calcium channel complex at a presynaptic nerve terminal: analysis by quantitative immunocolocalization, J. Neurosci. 24 (2004) 4070–4081.
[48] A. Luque, M. Gomez, W. Puzon, Y. Takada, F. Sanchez-Madrid, C. Cabanas, Activated conformations of very late activation integrins detected by a group of antibodies (HUTS) specific for a novel regulatory region (355–425) of the common beta 1 chain, J. Biol. Chem. 271 (1996) 11067–11075.
[49] M. Miyake, M. Koyama, M. Seno, S. Ikeyama, Identification of the motility-related protein (MRP-1), recognized by monoclonal antibody M31-15, which inhibits cell motility, J. Exp. Med. 174 (1991) 1347–1354.
[50] N. Ouchi, S. Kihara, S. Yamashita, S. Higashiyama, T. Nakagawa, I. Shimomura, T. Funahashi, K. Kameda-Takemura, S. Kawata, N. Taniguchi, et al., Role of membrane-anchored heparin-binding epidermal growth factor-like growth factor and CD9 on macrophages, Biochem. J. 328 (1997) 923–928.
[51] S. Ovalle, M.D. Gutierrez-Lopez, N. Olmo, J. Turnay, M.A. Lizarbe, P. Majano, F. Molina-Jimenez, M. Lopez-Cabrera, M. Yanez-Mo, F. Sanchez-Madrid, et al., The tetraspanin CD9 inhibits the proliferation and tumorigenicity of human colon carcinoma cells, Int. J. Cancer 121 (2007) 2140–2152.
[52] J.C. Porter, N. Hogg, Integrin cross talk: activation of lymphocyte function-associated antigen-1 on human T cells alters alpha4beta1- and alpha5beta1-mediated function, J. Cell Biol. 138 (1997) 1437–1447.
[53] M.J. Robertson, M.A. Caligiuri, T.J. Manley, H. Levine, J. Ritz, Human natural killer cell adhesion molecules. Differential expression after activation and participation in cytolysis, J. Immunol. 145 (1990) 3194–3201.
[54] J.L. Rodriguez-Fernandez, M. Gomez, A. Luque, N. Hogg, F. Sanchez-Madrid, C. Cabanas, The interaction of activated integrin lymphocyte function-associated antigen 1 with ligand intercellular adhesion molecule 1 induces activation and redistribution of focal adhesion kinase and proline-rich tyrosine kinase 2 in T lymphocytes, Mol. Biol. Cell 10 (1999) 1891–1907.
[55] J.L. Rodriguez-Fernandez, L. Sanchez-Martin, M. Rey, M. Vicente-Manzanares, S. Narumiya, J. Teixido, F. Sanchez-Madrid, C. Cabanas, Rho and Rho-associated kinase modulate the tyrosine kinase PYK2 in T-cells through regulation of the activity of the integrin LFA-1, J. Biol. Chem. 276 (2001) 40518–40527.
[56] M. Sala-Valdes, A. Ursa, S. Charrin, E. Rubinstein, M.E. Hemler, F. Sanchez-Madrid, M. Yanez-Mo, EWI-2 and EWI-F link the tetraspanin web to the actin cytoskeleton through their direct association with ezrin–radixin–moesin proteins, J. Biol. Chem. 281 (2006) 19665–19675.
[57] A. Salas, M. Shimaoka, A.N. Kogan, C. Harwood, U.H. von Andrian, T.A. Springer, Rolling adhesion through an extended conformation of integrin alphaLbeta2 and relation to alpha I and beta I-like domain interaction, Immunity 20 (2004) 393–406.
[58] F. Sanchez-Madrid, J.A. Nagy, E. Robbins, P. Simon, T.A. Springer, A human leukocyte differentiation antigen family with distinct alpha-subunits and a common beta-subunit: the lymphocyte function-associated antigen (LFA-1), the C3bi complement receptor (OKM1/Mac-1), and the p150,95 molecule, J. Exp. Med. 158 (1983) 1785–1803.
[59] P. Sanchez-Mateos, C. Cabanas, F. Sanchez-Madrid, Regulation of integrin function, Semin. Cancer Biol. 7 (1996) 99–109.
[60] J. Schindelin, I. Arganda-Carreras, E. Frise, V. Kaynig, M. Longair, T. Pietzsch, S. Preibisch, C. Rueden, S. Saalfeld, B. Schmid, et al., Fiji: an open-source platform for biological-image analysis, Nat. Methods 9 (2012) 676–682.
[61] C. Schmidt, V. Kunemund, E.S. Wintergerst, B. Schmitz, M. Schachner, CD9 of mouse brain is implicated in neurite outgrowth and cell migration in vitro and is associated with the alpha 6/beta 1 integrin and the neural adhesion molecule L1, J. Neurosci. Res. 43 (1996) 12–31.
[62] N. Shibagaki, K. Hanada, H. Yamashita, S. Shimada, H. Hamada, Overexpression of CD82 on human T cells enhances LFA-1/ICAM-1-mediated cell–cell adhesion: functional association between CD82 and LFA-1 in T cell activation, Eur. J. Immunol. 29 (1999) 4081–4091.
[63] T.N. Sims, M.L. Dustin, The immunological synapse: integrins take the stage, Immunol. Rev. 186 (2002) 100–117.
[64] P.M. Sincock, G. Mayrhofer, L.K. Ashman, Localization of the transmembrane 4 superfamily (TM4SF) member PETA-3 (CD151) in normal human tissues: comparison with CD9, CD63, and alpha5beta1 integrin, J. Histochem. Cytochem. 45 (1997) 515–525.
[65] O. Soderberg, M. Gullberg, M. Jarvius, K. Ridderstrale, K.J. Leuchowius, J. Jarvius, K. Wester, P. Hydbring, F. Bahram, L.G. Larsson, et al., Direct observation of individual endogenous protein complexes in situ by proximity ligation, Nat. Methods 3 (2006) 995–1000.
[66] T.A. Springer, M.L. Dustin, T.K. Kishimoto, S.D. Marlin, The lymphocyte function-associated LFA-1, CD2, and LFA-3 molecules: cell adhesion receptors of the immune system, Annu. Rev. Immunol. 5 (1987) 223–252.
[67] C.S. Stipp, T.V. Kolesnikova, M.E. Hemler, Functional domains in tetraspanin proteins, Trends Biochem. Sci. 28 (2003) 106–112.
[68] I. Tachibana, M.E. Hemler, Role of transmembrane 4 superfamily (TM4SF) proteins CD9 and CD81 in muscle cell fusion and myotube maintenance, J. Cell Biol. 146 (1999) 893–904.
[69] Y. Takeda, I. Tachibana, K. Miyado, M. Kobayashi, T. Miyazaki, T. Funakoshi, H. Kimura, H. Yamane, Y. Saito, H. Goto, et al., Tetraspanins CD9 and CD81 function to prevent the fusion of mononuclear phagocytes, J. Cell Biol. 161 (2003) 945–956.
[70] T. Tohami, L. Drucker, J. Radnay, H. Shapira, M. Lishner, Expression of tetraspanins in peripheral blood leukocytes: a comparison between normal and infectious conditions, Tissue Antigens 64 (2004) 235–242.
[71] Y. van Kooyk, C.G. Figdor, Avidity regulation of integrins: the driving force in leukocyte adhesion, Curr. Opin. Cell Biol. 12 (2000) 542–547.
[72] Y. van Kooyk, P. van de Wiel-van Kemenade, P. Weder, T.W. Kuijpers, C.G. Figdor, Enhancement of LFA-1-mediated cell adhesion by triggering through CD2 or CD3 on T lymphocytes, Nature 342 (1989) 811–813.
[73] Y. van Kooyk, E. van de Wiel-van Kemenade, P. Weder, R.J. Huijbens, C.G. Figdor, Lymphocyte function-associated antigen 1 dominates very late antigen 4 in binding of activated T cells to endothelium, J. Exp. Med. 177 (1993) 185–190.
[74] T.S. van Zanten, A. Cambi, M. Koopman, B. Joosten, C.G. Figdor, M.F. Garcia-Parajo, Hotspots of GPI-anchored proteins and integrin nanoclusters function as nucleation sites for cell adhesion, Proc. Natl. Acad. Sci. U. S. A. 106 (2009) 18557–18562.
[75] S.E. VanCompernolle, S. Levy, S.C. Todd, Anti-CD81 activates LFA-1 on T cells and promotes T cell–B cell collaboration, Eur. J. Immunol. 31 (2001) 823–831.
[76] I. Weibrecht, K.J. Leuchowius, C.M. Clausson, T. Conze, M. Jarvius, W.M. Howell, M. Kamali-Moghaddam, O. Soderberg, Proximity ligation assays: a recent addition to the proteomics toolbox, Expert Rev. Proteomics 7 (2010) 401–409.
[77] M. Yanez-Mo, O. Barreiro, M. Gordon-Alonso, M. Sala-Valdes, F. Sanchez-Madrid, Tetraspanin-enriched microdomains: a functional unit in cell plasma membranes, Trends Cell Biol. 19 (2009) 434–446.
[78] M. Yanez-Mo, A. Alfranca, C. Cabanas, M. Marazuela, R. Tejedor, M.A. Ursa, L.K. Ashman, M.O. de Landazuri, F. Sanchez-Madrid, Regulation of endothelial cell motility by complexes of tetraspan molecules CD81/TAPA-1 and CD151/PETA-3 with alpha3 beta1 integrin localized at endothelial lateral junctions, J. Cell Biol. 141 (1998) 791–804.
[79] R.L. Yauch, M.E. Hemler, Specific interactions among transmembrane 4 superfamily (TM4SF) proteins and phosphoinositide 4-kinase, Biochem. J. 351 (Pt 3) (2000) 629–637.